Università degli Studi di Napoli "Federico II"

PhD program in "Scienze Agrarie e Agroalimentari"
XXIX ciclo

Glutamate binding protein: A novel SBP

for future biosensor development

Tutor:
Prof. Danilo Ercolini
Co-Tutor Sabato D'Auria

Candidate:

Dott. Stefano Di Giovanni

Coordinator:
Prof. Guido D'Urso

Anno 2017

Index

ABBREVIATIONS

ABC: ATP-binding cassette
ANS: 8-anilino-1-naphthalenesulfonic acid
CAPS: N-cyclohexyl-3-aminopropanesulfonic acid
CD: Circular Dichroism
DEAE: diethylaminoethanol
ECL: enhanced chemiluminescence
FRET: Fluorescent Resonance Energy Transfer
IEC: ion-exchange chromatography
LMW: Low Molecula weight
MRE: Molecular Recognition Element
MSG: mono sodium L-glutamate
MW: Molecula weight
NMR: Nuclear Magnetic Resonance
ORF: Open Reading Frame
SDS/Native PAGE: Sodium Dodecyl Sulphate/Native - PolyAcrylamide Gel Electrophoresis
PCR: Polymerase Chain Reaction
PBPs: Periplasmic Binding Proteins
PVDF: polyvinylidene difluoride
RT: Room Temperature
SBPs: Substrate-binding proteins
Far-UV: Far ultraviolet
WB: Western blot
LBR: Ligand Binding Region
GluB-lP/P: GluB-lipoprotein /His-Tag protein

Abstract:

Substrate-binding proteins (SBPs), members of a protein superfamily, are suitable to be used as molecular recognition elements (MRE) for biosensor development (Dwyer & Hellinga 2004). Their main function is to transport various biomolecules such as sugars, amino acids, peptides and inorganic ions into the cell (Tian *et al*. 2007). Although these proteins vary in term of size and primary sequence, they have similar tertiary structures. In particular, the three-dimensional structures consist of two domains linked by a hinge region and the ligand-binding site is located at the interface between the two domains (Dattelbaum & Lakowicz 2001). In Gram-positive bacteria SBPs are either anchored to the cytoplasmic membrane or fused to membrane-anchored domains of ATP-binding cassette (ABC) importers (Berntsson *et al*. 2010). SBPs are highly specific for a wide range of analytes, which bind even in nano-molar concentrations. Moreover SBPs undergo a ligand-induced conformational change that can be detected by variations of optical properties of protein structural features such as fluorescence intensity emission (Grunewald 2014). These properties allow the use of SBPs to construct optical and electrochemical biosensors for a wide variety of chemical classes, including sugars, amino acids, dipeptides, cations and anions. Therefore this class of proteins is widely used as probes for reversible optical sensors of analytes with high social impact. An example of SBP is the Glutamate-binding Protein (GluBP) that is a potential candidate as MRE for a biosensor to detect glutamate. GluBP is a lipoprotein isolated from *Corynebacterium glutamicum* in which is involved in glutamate uptake. *Corynebacterium glutamicum* is a Gram-positive, facultative anaerobic, heterotrophic bacterium, which belongs to the mycolic acid-containing actinomycetes. It is not pathogenic and it can be found in soil, animal faeces, fruits and vegetables (Trötschel *et al*. 2003). Moreover, *Corynebacterium glutamicum* is very important bacterium involved in monosodium glutamate (MSG) industrial production. It is able to produce large amounts of glutamate, but its uptake carriers allow it to exploit L-glutamate as unique nitrogen and carbon source hence, this bacterium can grow on a minimal medium (Burkovski *et al*. 2003). Genetic engineering gives the possibility to manipulate genes to modulate the affinity and selectivity of proteins. This allows us to greatly expand the range of biochemically relevant analytes, which can be measured by protein-based sensors. In this context, we studied the possibility to develop a fast and stable glutamate biosensor using Glutamate-binding Protein (GluBP). Recently, crystals of GluBP were obtained but the 3D structure to be resolved by X-Ray crystallography (Liu *et al*. 2013). In order to expand knowledge on this SBP, the project of thesis is focalized on the functional and structural characterization of GluB-lipoprotein /His-Tag protein (GluB-lP/P). In particular GluB-lP/P from *C. glutamicum* was deeply studied for the understanding

of its structural properties by Fluorescence Spectroscopy and Circular Dichroism. By these techniques, the effect of temperature on the stability of the protein, other chemico-physical perturbation (such as pH and presence of cations) of the intrinsic two fluorescence tryptophan residues were investigated in the absence and in the presence of L-glutamate. Obtained results show that L-glutamate stabilises GluBP secondary and tertiary structures increasing Temperature of melting about 10 °C. Sodium ions increase the thermal stability. Thermal stability increases at pH 8. In addition, L-glutamate binding experiments allowed the calculation of apparent binding Kostant (Kd) of about 6 nM. L-glutamate binding, induces blue-shift in fluorescence spectra from 337 up to 331 nm as happens by reducing the pH from pH 8 to pH 6. Acrylamide fluorescence quenching at pH 8 in the presence of L-glutamate have confirmed that GluBP changes the tertiary structure and tryptophans became buried. In addition GluBP binding experiments were also performed in the presence of L-glutamine and L-aspartate and only in the presence of L-aspartate was possible to obtain a partial increase of thermal stability, which confirmed the specificity of GluBP for L-glutamate. In the near future, the resolution of X-Ray 3D structure of GluBP will allow obtain structural information for GluBP engineering that will allow the development of a fluorescent biosensor against L-glutamate in food, tears, blood sweat and so on.

Introduction

## Substrate-binding proteins for biosensor development

SBPs are members of a protein superfamily that are suited as MRE for the biosensors engineering (Dwyer & Hellinga 2004). Their main function is to transport various biomolecules such as sugars, amino acids, peptides and inorganic ions to the cell (Tian *et al*. 2007). Although these proteins differ in size and primary sequence, they have similar structures. In particular, the three-dimensional structure consists of two domains linked by a hinge region, and the ligand-binding site is located at the interface between the two domains (Dattelbaum & Lakowicz 2001, Roland *et al*. 1993). In Gram-positive bacteria, the SBPs are either anchored to the cytoplasmic membrane with a lipid anchor (such as a palmilate) or fused to membrane-anchored domains of ABC importers (Berntsson *et al*. 2010, Gilson *et al*. 1988, Schneider *et al*. 1993, Sutcliffe *et al*. 1993 and Sutcliffe *et al*. 1995, Alloing *et al*. 1994, Chang *et al*. 1994, Jenkinson *et al*. 1996). Several lines of evidence for the structure of GluBP of *C. glutamicum* are in accord with the view that in gram-positive bacteria the binding proteins are lipoproteins. First of all, a signal sequence with a basic region at the N terminus carrying three positive charges followed by a stretch of hydrophobic and apolar residues are present. Such a structure is characteristic of signal sequences (Jenkinson *et al*. 1996).

In Gram-negative bacteria that have an outer membrane, the SBPs are usually found in the periplasmic place and are denominated Periplasmic Binding Proteins (PBPs). They bind their substrate and transport it by trans-membrane transporters. An example of PBP is the Arginine-Binding protein (ArgBP) that is responsible for the first step in the active transport of L-arginine across the cytoplasmic membrane and important role in regulation of intracellular arginine concentration (Ausili *et al*. 2013). In Figure 1, a 3D cartoon models of TmArgBP in the absence (A) and in the presence (B) of arginine (displayed in spheres). The ligand-binding induces the bending of the two domains that makes the protein assumes the closed form (Ausili *et al*. 2013).

The SBPs are highly specific for a wide range of analytes. They bind even in nano-molar concentrations and undergo a ligand-induced conformational change that can be detected by changes in optical properties of the protein, such as fluorescence intensity (Grunewald 2014) or lambda max of emission of fluorescence (Dattelbaum & Lakowicz 2001). Moreover, these biosensors allow analyte-detection without chemical reaction (Grunewald 2014). These properties allow using SBPs to construct reagentless optical and electrochemical biosensors for a wide variety of chemical classes, including sugars, amino acids, dipeptides, cations and anions.

Figure 1 Structure of SBP in the absence (A) and in the presence (B) of substrate (Ausili *et al.* 2013)
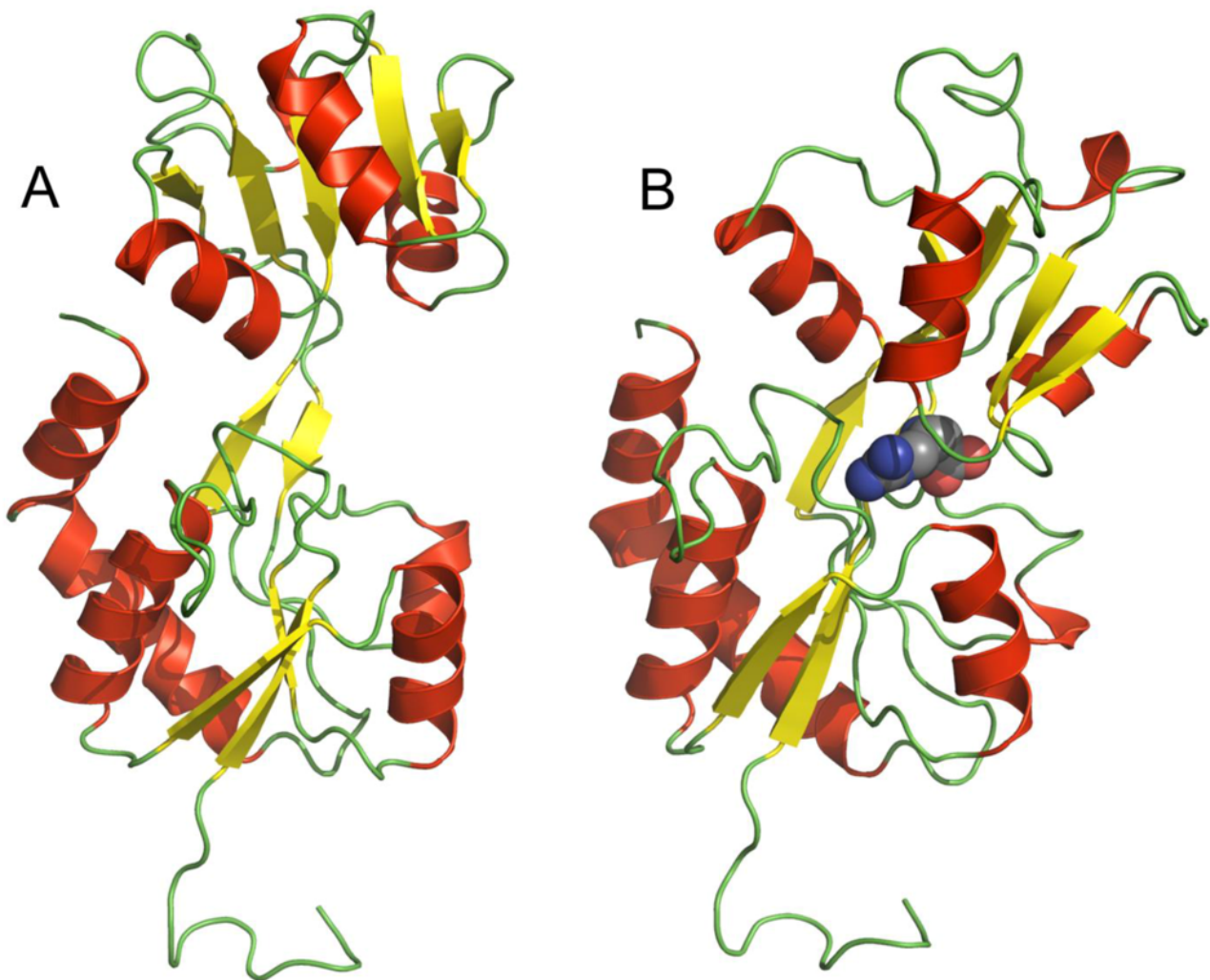
Glutamate-binding protein in *Corynebacterium glutamicum*

The SBPs, together with ABC proteins and permeases in the inner membrane of bacteria (gram-negative bacteria such as *E. coli*) or plasma membrane in Gram-positive bacteria (such as *C. glutamicum*), are involved in the active transport of various water-soluble ligands (Tam & Saier 1993, Boos & Lucht 1996). They bind such ligands as monosaccharides, oligosaccharides, amino acids, oligopeptides, sulfate and phosphate in the periplasmic space or outside plasma membrane in gram-negative bacteria, and interact with membrane components. The ABC proteins drive the transfer of ligands through permeases by hydrolysis of ATP. Although this transport system was originally found in Gram-negative bacteria, the genes for this system have also been discovered in other bacteria without a periplasmic space, such as gram-positive *Mycoplasma* (Gilson *et al.* 1988), cyanobacteria (Montesinos *et al.* 1997), archaebacteria (Klenk *et al. 1997*), and Corynebacteria (from the Greek words *koryne,* meaning club, and *bacterion,* meaning little rod). Overview of

putative or verified peptide and amino acid transport systems of *C. glutamicum* based on the genome annotation and available literature (GluBP: Cg2137 or NCgl1876-) (Michel *et al.* 2015). *Corynebacterium glutamicum* is a Gram-positive, facultative, anaerobic and heterotrophic bacterium, which belongs to the mycolic acid-containing actinomycetes. It is not pathogenic and it was found in soil, animal faeces, fruits and vegetables (Trötschel *et al.* 2003). Coryneform bacterium, *Corynebacterium glutamicum*, was isolated as an L-glutamate-overproducing microorganism by Japanese researchers and is currently utilized in various amino acid fermentation processes. L-glutamate production by *C. glutamicum* is induced by limitation of biotin and addition of fatty acid ester surfactants and β-lactam antibiotics. These treatments affect the cell surface structures of *C. glutamicum* (Hirasawa & Wachi 2016). After the discovery of *C. glutamicum*, many researchers have investigated the underlying mechanism of L-glutamate overproduction with respect to the cell surface structures of this organism. Furthermore, metabolic regulation during L-glutamate overproduction by *C. glutamicum*, particularly, the relationship between central carbon metabolism and L-glutamate biosynthesis, has been investigated (Hirasawa & Wachi 2016). *C. glutamicum* is not only able to produce large amounts of glutamate, but this organism possesses even uptake carriers that allow it to grow on L-glutamate as unique nitrogen and carbon source. The high-affinity of the glutamate uptake system *C. glutamicum* is typical of binding protein-dependent systems. In this way, the bacterium can grow on a minimal medium (Burkovski *et al.* 1996).

SBPs vary in size from roughly 25-70 kDa, and despite little sequence similarity their overall three-dimensional structural fold is highly conserved. The crystal structures of more than a dozen SBPs have been determined with high-resolution to elucidate the atomic interactions associated with the specific recognition and binding of a variety of ligands.

GluBP is a lipoprotein consisting of 295 amino acid residues and with a molecular weight of 29 KDa. At the N-terminal end, there are 26 amino acid residues that have been identified as signal sequence: they are responsible for protein translocation through the cytoplasmic membrane. (Kronemeyer 1995). According to different evidence, it is thought that GluBP is a lipoprotein (Poetsch & Wolters 2008) (Kronemeyer 1995).. The signal sequence in the N-terminal end carries three positive charges followed by hydrophobic and apolar residues. The hydrophobic core is followed by the short sequence LTACGD that is the target of a signal peptidase II. Moreover, there is a glycerol-cysteine lipid residue of GluBP that is responsible for anchoring the binding protein in the membrane. As all SBPs, GluBP is part of ABC transporters and, together with the trans-membrane proteins GluC and GluD and the cytoplasmic protein GluA, forms a highly active glutamate uptake system that aims to couple the hydrolysis of ATP to the translocation of glutamate. The primary glutamate uptake is encoded by a gluABCD gene cluster that

comprises an ATP-binding protein, encoded by gluA, and Glutamate binding protein, encoded by gluB gene, and two integral membrane proteins, encoded by gluC and gluD (Kronemeyer 1995). GluBP is a lipoprotein anchored to the plasma membrane of *C. glutamicum* and at moment is only present a crystal (See Figure 3) and a 3D structure of crystal is not resolved (Liu *et al*. 2013). SBP of *Corynebaxterium glutamicum*, Glutamate-binding lipoprotein (GluBlP), is a small (28.7 kDa), soluble protein belonging to the large family of specific binding proteins that are essential primary receptors in transport various biomolecules, such as sugars, amino acids, peptides, and inorganic ions. (Qin *et al*. 2013, Kaivosoja *et al*. 2015, Hosseini *et al*. 2014) Although these proteins range in size and primary sequence, they have remarkably similar topology (Hires *et al*. 2008, Liu *et al*. 2013). GluB lipoprotein has 32% of sequence identity with antigen peb1a from *Campylobacter jejuni*, an aspartate and glutamate-binding protein since sequence diversity within the superfamily is high, but the general structural fold is conserved on basis of this protein structure; PDB entry: 2V25 (Berman *et al*. 2000) allowed as to obtain a three-dimensional structure and a representative 3D cartoon structure of GluB lipoprotein (Figure 2B).

Figure 2: Template Structure antigen peb1a vs Target Sequence of GluBP
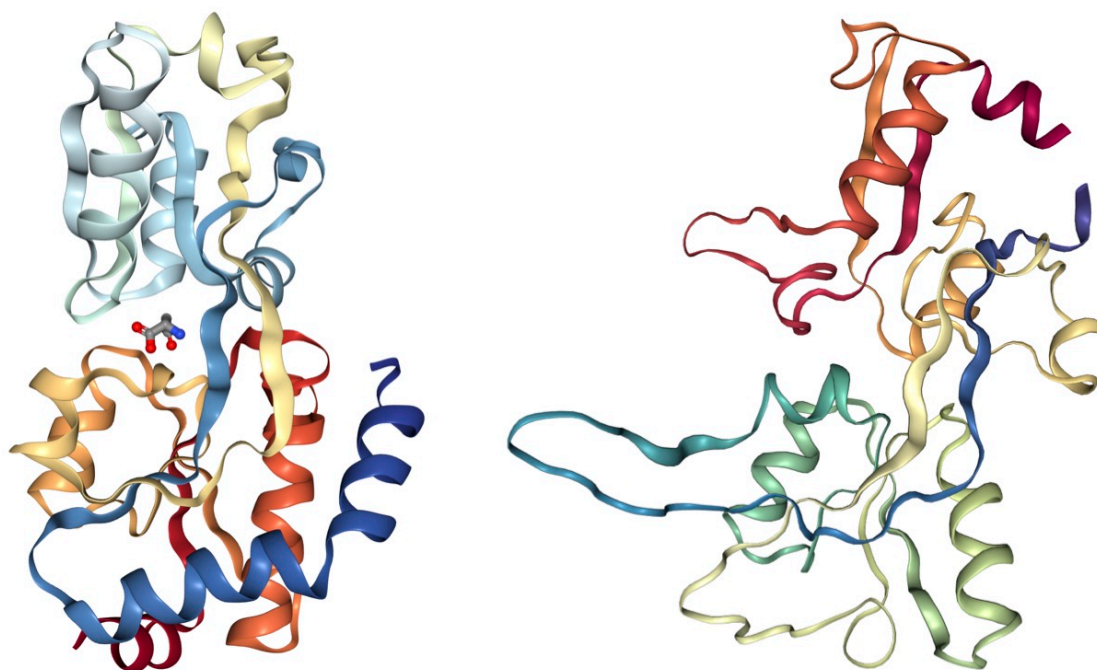
Template Structure: The structure of the *Campylobacter jejuni* antigen peb1a, an aspartate and glutamate receptor with bound aspartate.

Target Sequence: The structure of the ABC-type glutamate transporter, substrate-binding lipoprotein GluB lipoprotein in the absence of glutamate.

In Figure 2 on the left structure (PDB: 2V25) an aspartate and glutamate receptor with bound aspartate; on the right a representative 3D model of GluB lipoprotein. This model is based on target-template sequence alignment of 32% sequence identity between two SBP. (ModBase: Database of Comparative Protein Structure Models). Cartoon structures were obtained using the NGL Viewer (Rose & Bradley 2016, Rose & Hildebrant 2015). In fact, In spite of large sequence-length variation and low sequence identity, they share common features of three-dimensional structure and patterns of ligand-binding as follows (Davidson *et al.* 2008): i) SBPs consist of two globular domains of mainly α/β type connected by a hinge region mainly β type, with a ligand-binding site located at the interface between the two domains, which can adopt two different conformations (Figure 4); ii) the ligand is bound in a ligand-binding site located at the interface between the two domains and engulfed by both, with a ligand-free open form and a ligand-bound closed form, which interconvert through a relatively large bending motion around the hinge; iii) a hinge-bending motion between the two domains is accompanied by ligand-binding (Quiocho 1991, Quiocho & Ledvina 1996), which interconvert through a relatively large bending motion around the hinge.

Figure 3 Crystals of GluBP from *C. glutamicum* from Liu *et al*. 2013 (A) and Einspahr *et al*. 2014 (B)
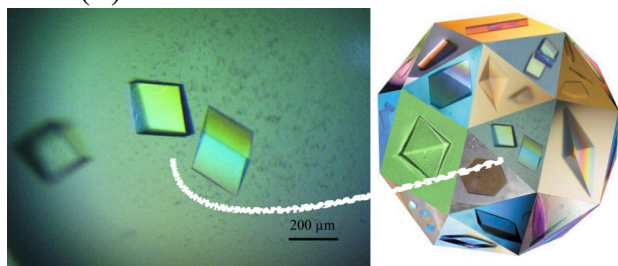
A   **B**

Substrates binding stabilize a closed conformation of the proteins in which the domains are tightly packed together with the substrate buried at the interface (Ooij *et al*. 2009). All these features imply that SBPs originated from a common ancestor (Dwyer & Hellinga 2004).

The diversity of biological function, ligand-binding, conformational changes and structural adaptability of the Substrate-binding protein superfamily have been exploited to engineer biosensors (Dwyer & Hellinga 2004). Protein recognition-based biosensors are projected to find many research, clinical, industrial, and environmental and security applications in the near future. In medical and clinical field or research in cellular biology, protein-based biosensor is crucial for analyte monitoring of relevant in diagnosis and the follow-up of high social interest pathology (Alzheimer Disease, Parkinson Disease, etc.). In industrial field, protein-based biosensor can be used for analyte release control and in particular to accurately and reliably measure of glutamate release in bacterial fermentation such as *C. glutamicum* fermentations in different scales. An example of SBP is the Glutamate-binding lipoprotein (GluB-lP). As new MRE, it is potential candidate for a biosensor to detect glutamate. GluBP is a lipoprotein involved in glutamate uptake and isolated in *C. glutamicum*.

The aim of this project is to study the Glutamate-binding protein from an anaerobic and heterotrophic bacterium *C. glutamicum* to develop a protein-biosensor based that is able to bind glutamate. As new MRE, it is potential candidate for a biosensor to detect glutamate. GluBP is a lipoprotein involved in glutamate uptake and isolated in *C. glutamicum*. The L-glutamate binding lipoprotein (GluB-lP), as many other SBP, is the initial component of glutamate transport of ABC transporter system in *C. glutamicum*, upon glutamate-binding undergo a large conformational change in two globular domain to accommodate the ligand inside the binding site as shown in Figure 4 (Berntsson *et al*. 2010).

Figure 4: Open and close conformation of SBP-binding site: slice through surface representation of OppA structure from *L. lactis* from Ooij *et al.* 2009 (A). Ball-and-stick model of L-glutamate (B)

A   **B**
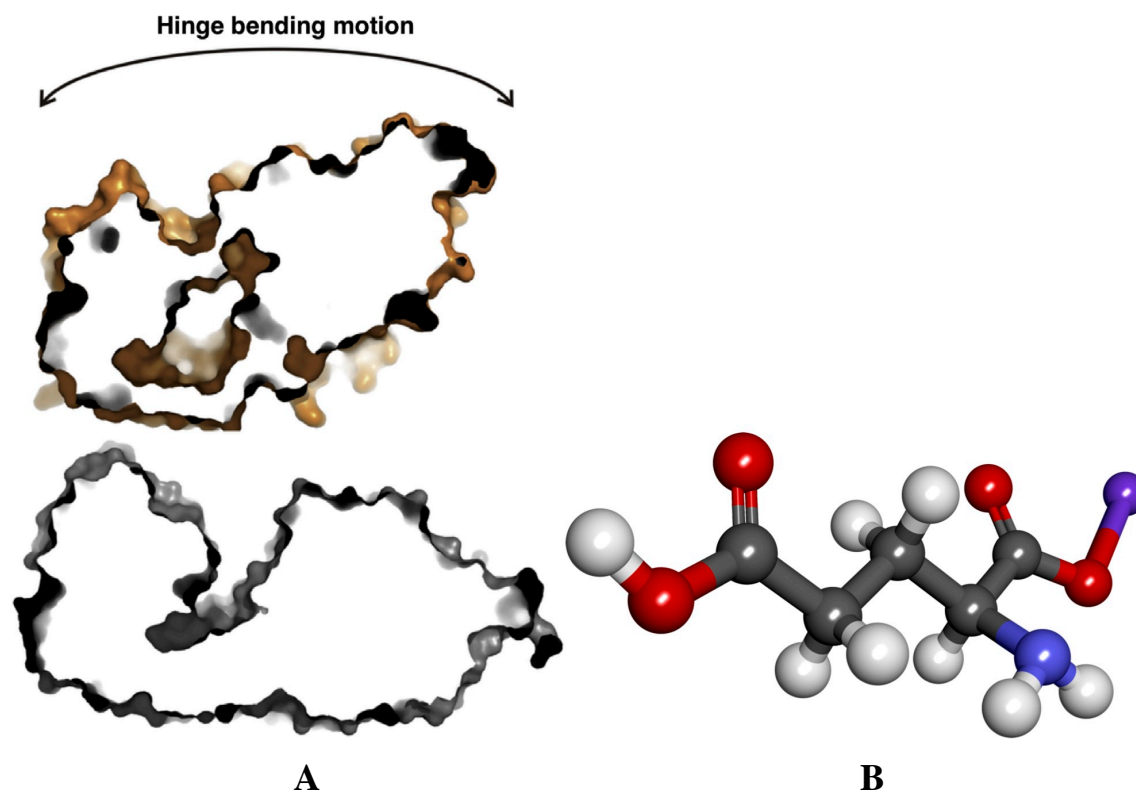
Based on this conformational change, sensing system for glutamate can be developed. Knowledge of the details of structural properties as well as the conformational stability of GluB lipoprotein /protein (GluB-lP/P) is needed when developing biotechnological applications. Besides information on the basic knowledge, the new insights on GluBP constitute important data for the development of those biotechnological applications requiring detailed information on the protein structural-functional properties as in the case of manipulation of the protein to use as probe for a biosensor for glutamate monitoring in different fields and with different properties, as is shown in Figure 8 and future application of GluB-lP/P for fluorescent FRET-based biosensor.

Spectroscopic Characterization of Glutamate-binding protein as potential Molecular Recognition Element

The structural and functional characterization of GluBP has been done using advanced spectroscopy techniques. Circular Dichroism (CD) and Fluorescence Spectroscopy are used to investigate GluBP secondary structure and tertiary structure, respectively in the presence and in the absence of the glutamate. The CD is considered a viable technique to study the structure of proteins in solution

(Chen *et al*. 1974). Unlike the crystallography and NMR, that are other techniques that provide structural information, CD is a low-resolution structural technique in which overall structural features are described. However, it is less demanding in terms of time and sample in fact reliable spectra are obtained using low quantities of protein (0.1 mg).

It also allows to explore the protein structure in different conditions and to monitor the structural changes when the micro-environmental changes. The spectro-polarimeter measures the differential absorption of circularly polarised components, Left (L) and Right (R) handed light, and report this difference in terms of ellipticity (θ) expressed in degree. The chromophores that allow for a CD signal are: i) peptide bonds that absorb below 240 nm and consent to define the secondary structure of a protein (Far-UV); ii) aromatic amino acid side chains that absorb in the range 260 to 320 nm and give information on tertiary structure of protein (Near UV). The switch between α-helical and β-sheet structures can indicate the ligand-binding to a protein. This structural change can be detected by CD signals. The CD signals at 208 nm and 222 nm estimate the α-helix content of protein. Moreover, the loss of CD signals by adding denaturing agents or by increasing temperature indicates the stability of the protein (Kelly *et al*. 2005).

The proteins can be used as intrinsic fluorescence probe because the three aromatic amino acids, tryptophan (W, Trp), tyrosine (Y, Tyr) and phenylalanine (F, Phe) are all fluorescent, although with different intensities. Protein fluorescence is generally excited at the absorption maximum near at 280 nm and so the phenylalanine does not contribute to protein fluorescence. The absorption at 280 nm is due to tyrosine and tryptophan, but at wavelength longer than 295 nm, the absorption is primarily due to tryptophan. Thus, it is possible to select tryptophan fluorescence by exciting at 295-305 nm. Through fluorescence of protein it is possible investigate the conformational transitions, subunit associations, substrate-binding or denaturation because of the high sensitivity of tryptophan to the local environment. Some quenchers of tryptophan fluorescence, as lysine and histidine residues and in certain conditions even amide groups of the protein backbone, can act as quencher. For this reason, by tryptophan fluorescence, it is possible to obtain information on the tertiary structure of the protein (Lakowicz 2006). Moreover indication on quaternary structure by size exclusion chromatography (SEC) of GluBP might indicate that GluBP forms dimers. All these structural information are new key elements for developing glutamate fluorescence biosensor with GluBP as MRE.

## Glutamate's Role in Mammalian Central Nervous System

L-glutamate is one of the major amino acids that are present in a wide variety of foods. It is mainly used as a food additive and flavour enhancer (umami) in the form of sodium salt; in Figure 4B is showed the L-monosodium glutamate structure. The amino acid L -glutamate is considered to be the major mediator of excitatory signals in the mammalian central nervous system and is probably involved in most aspects of normal brain function including cognition, memory and learning (Fonnum 1984, Ottersen & Storm –Mathisen 1984, Collingridge & Lester 1989, Headley & Grillner 1990). Glutamate also plays major roles in the development of the central nervous system, including synapse induction and elimination, and cell migration, differentiation and death. Most neurons and even glial cells have glutamate receptors in their plasma membranes (Hösli & Hösli 1993, Steinhäuser & Gallo 1996, Vernadakis 1996, Conti *et al*. 1999, Shelton & McCarthy 1999, Bergles *et al*. 2000). Brain glutamate is abundant, but mostly intracellular. The brain contains huge amounts of glutamate (about 5– 15 mmol per kg wet weight depending on the region) (Schouboe & Hertz 1981), but only a tiny fraction of this glutamate is normally present in extracellular part of cell (outside or between the cells). Consequently, the concentration gradient of glutamate across the plasma membranes is several thousand-fold. The highest concentrations are found inside nerve terminals (Ottersen *et al*. 1992, Mathisen *et al*. 1992, Ottersen *et al*. 1996); glutamate is continuously being released from cells and is continuously being removed from the extracellular fluid. Glutamate exerts its signalling role by acting on glutamate receptors. Therefore it is the glutamate concentration in the surrounding extracellular fluid that determines the extent of receptor stimulation. It is of critical importance that the extracellular glutamate concentration is kept low. This is required for a high signal-to-noise (background) ratio in synaptic as well as in extra-synaptic transmission. The concentrations in the extracellular fluid, which represents 13-22% of brain tissue volume, and in the cerebrospinal fluid (CSF) (Danbolt 2001) are normally around 3-4 μM and around μ10 M, respectively (Lehmann & Hamberger *et al*. 1983; Lehmann *et al*. 1983; Hamberger and Nyströ *et al*. 1984). The transporter proteins represent the only (significant) mechanism for removal of glutamate from the extracellular fluid and their importance for the long-term maintenance of low and non-toxic concentrations of glutamate is now well documented. Further, the glutamate transporters provide glutamate for synthesis of e.g. g-aminobutyric acid (GABA), glutathione and protein, and for energy production. In fact L-glutamate is the precursor of the inhibitory neurotransmitter g-aminobutyric acid (GABA) and neither the normal functioning of glutamatergic synapses nor the pathogenesis of major neurological diseases (e. g. cerebral ischemia, hypoglycaemia, amyotrophic lateral sclerosis, Alzheimer's disease, traumatic brain injury, epilepsy and schizophrenia) (Danbolt 2001) as well as non-neurological diseases (e. g. osteoporosis). It has

also been noted that glutamate levels are increased in a damaged brain (Hamdam & Mohd Zain 2014). Glutamate, as a neurotransmitter, is involved in different physiological processes: brain development, neurotransmission, synaptic plasticity and neurotoxicity. Further, glutamate plays a signalling role also in peripheral organs and tissues as well as in endocrine cells (Moriyama *et al*. 2000). Further, excessive activation of glutamate receptors is harmful, and glutamate is thereby toxic in high concentrations In contrast, intracellular glutamate is generally considered non-toxic, but it should be kept in mind that intracellular glutamate may not be completely inert (Danbolt 2001). Although it is toxic, L -glutamate is important because it not only mediates substantial information, but also regulates brain development: it determines cell survival, the differentiation, the formation and the elimination of synapses. Glutamate, as an amino acid, facilitates both amino acid synthesis and degradation. In liver it is the terminus for the release of ammonia from amino acid and the intrahepatic concentration of glutamate modulates the rate of ammonia detoxification into urea; in pancreatic beta-cells, oxidation of glutamate mediates amino acid stimulated insulin secretion (Kelly *et al*. 2005).

The amino acid L-glutamate (Fig. 4B) is considered to be the major mediator of excitatory signals in the mammalian central nervous system and is probably involved in most aspects of normal brain function including cognition, memory and learning (Fonnum *et al*. 1984; Ottersen & Storm-Mathisen *et al*. 1984; Collingridge & Lester 1989; Headley & Grillner 1990). Glutamate must be present in right concentration, in the right time and in the right place because, both too much and too little, glutamate is harmful (Hamdan & Mohd Zain 2014). Only cells with glutamate receptors on their surfaces are sensitive to glutamate; there are glutamate receptors in most of nerve and glial cells. Glutamate acts post-synaptically on three families of ionotropic receptors (NMDA, AMPA and Kainate) that are ion channels permeable to cations. Interestingly the glutamate recognition sites within show sequence similarity with bacterial SBP. Sensitive sequence analysis techniques indicate that the metabotropic receptor extracellular domain is similar to bacterial periplasmic amino acid binding proteins (O'Hara *et al*. 1993). The extracellular region is further divided into the ligand- binding region (LBR) and the cysteine-rich region. The mGluR structure is divided into three regions: the extracellular region, the seven-spanning trans-membrane region and the cytoplasmic region (See Figure 6A). LBR has sequence similarity to the leucine/isoleucine/valine-binding protein (LIVBP), which is a bacterial periplasmic binding protein (O'Hara *et al*. 1993) as shown in Figure 6B (modified by Berntsson *et al*. 2006), as well as to the extracellular regions of both iGluR7 and the GABA B receptor (Kaupmann *et al*. 1997).

Figure 5: Summary diagram of the processes in neurons and astrocytes which have been shown to, or could in principle contribute, to the rise in [Glu] and [Ca²⁺] (Rossi *et al.* 2007)
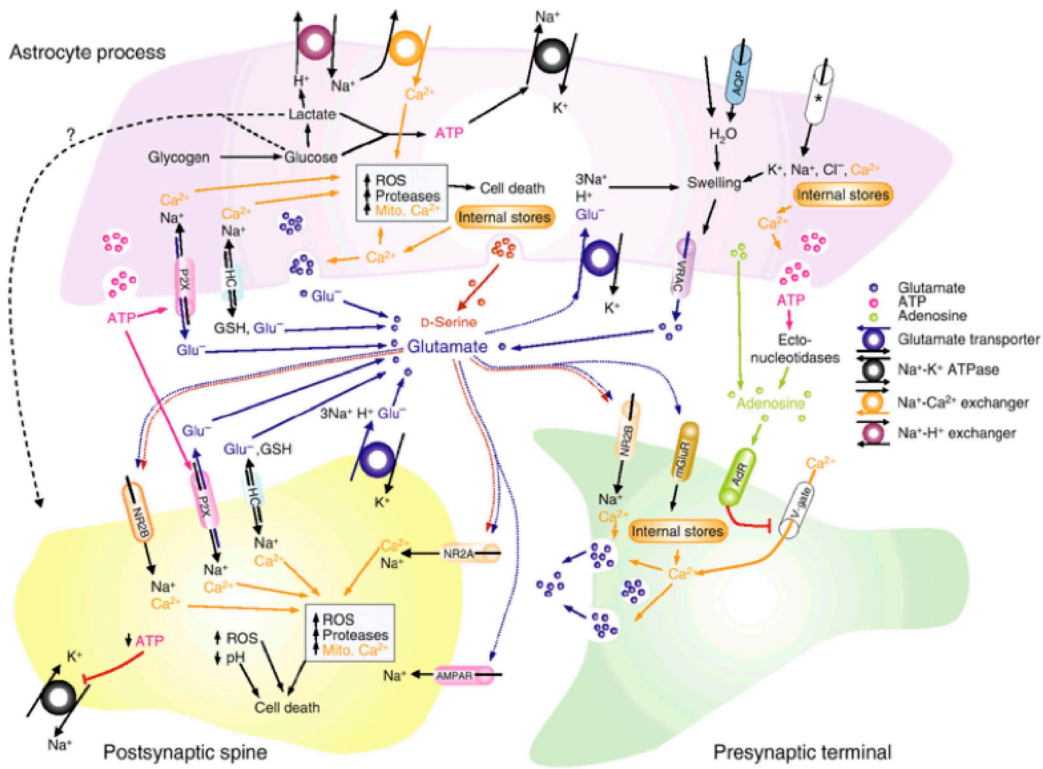
Figure 6: General structure of metabotropic glutamate receptors *versus* ABC importers (Sung *et al.* 2007) e.g. for analytes such as glutamate. Red row indicates direction of glutamate entry thought bacterial membrane protein

A   B
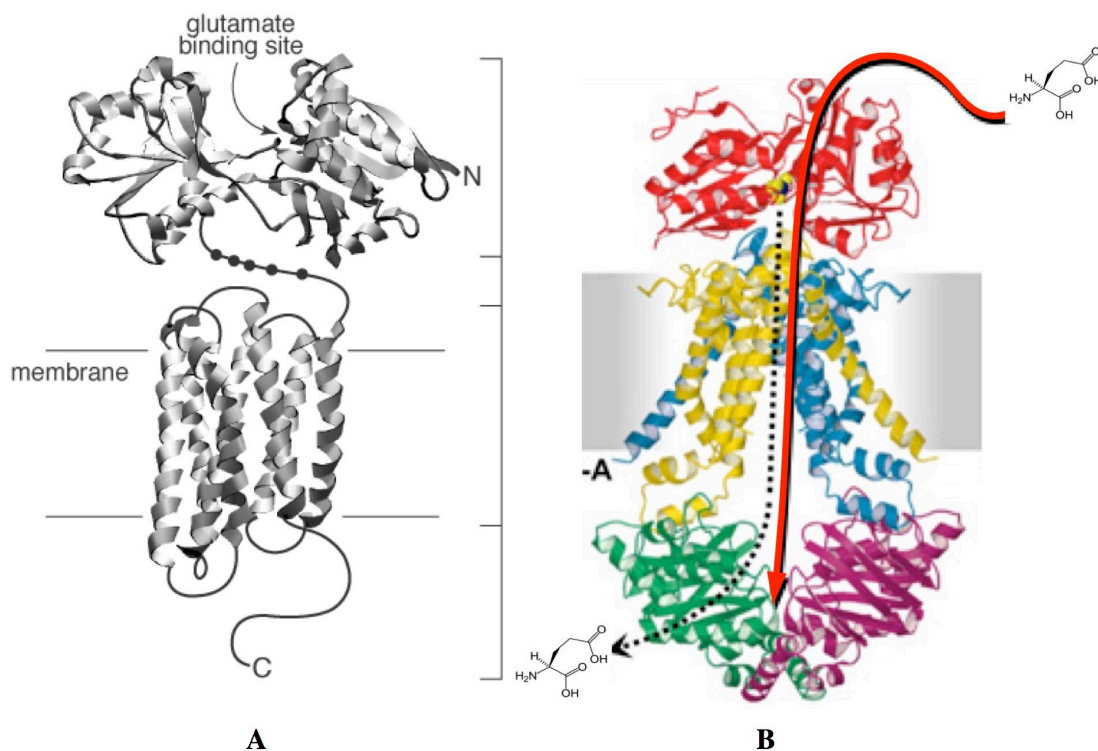
Glutamate is almost exclusively located inside cells: the intracellular location is of approximately 99.99%. This is essential because glutamate receptors can only be activated by extracellular glutamate, so glutamate is relatively inactive if it is intracellular. When glutamate is released normally in the synaptic cleft, its concentration increases to 1 mM, but it remains for a few milliseconds at this concentration (Hamdan & Mohd Zain 2014). Glutamate is released in presynaptic terminals through a Ca^{2+}-dependent mechanism and this produces an excitatory postsynaptic potential (EPSP) that is related to receptors activation. Astrocytes uptake glutamate released from synapses and here it is converted into glutamine. The latter is released to be re-uptaken from neurons and it is used to regenerate glutamate.

This glutamate-glutamine shuttle (See Figure 5) is essential to avoid toxic extracellular accumulations of glutamate (Kelly & Stanley 2001). Another way to remove glutamate from synaptic cleft is through high-affinity Na^+-dependent transporters, that are membrane proteins with eight putative trans-membrane domains that use Na^+/K^+ electrochemical gradients as a driving force across the plasma membrane (Soldatkin *et al*. 2015).

### Glutamate As Enhancer of Flavour and Excitotoxicity

MSG is widely used as an enhancer of flavour in foodstuff, such as soups, sauces and seasonings. It represents a unique taste denominated "umami" that is considered as the fifth taste. The optimal concentration of glutamate that humans can take is between 0.2% and 0.8%. The ingestion of high concentrations of glutamate can cause headache, numbness and palpitation. These symptoms are described as MSG Symptom Complex (Muslima *et al*. 2012). Excitotoxicity is the pathological process by which neurons are damaged and killed by the excessive activations of excitatory neurotransmitter glutamate receptors (Hamdan & Mohd Zain 2014). An excessive amount of extracellular glutamate causes overstimulation of receptors with a consequent increase of calcium thorough NMDA entry (Soldatkin *et al*. 2015). High concentrations of calcium activate several enzymes that contribute to cell death: proteases, phospholipases, nitric oxide synthetases or nucleases (Sundaram *et al*. 2012). It is possible to recognize three different mechanisms involved in the glutamate excitotoxicity: i) consumption of exogenous glutamate from the diet; ii) endogenous glutamate released from neurons can contribute to acute neurodegeneration in presence of cerebral ischemia or traumatic brain injury; iii) glutamate receptors activation can cause cell death in chronic neurodegenerative disorders (Meldrum 2000).

Biosensors

A biosensor is a self-contained integrated device that is capable of providing specific quantitative or semi-quantitative analytical information using a biological recognition element (bio-receptor),

which is in direct spatial contact with a transducer element. In last decade, biosensors have proved to be extremely reliable tools as a complement and, in some cases, such as replacement of existing analytical methodologies in the detection and monitoring of environmental, medical, food safety and homeland securities analytes. Biosensors are classified on the basic principles of signal transduction and bio-recognition elements. In fact, according to the transducing elements, biosensors can be classified as electrochemical (potentiometric, amperometric and conductometric biosensors), optical, piezoelectric, and thermal biosensors. On the other hand, based on the bio-receptor used, it is possible to classify the biosensor and in particular, in the case of protein-based biosensors, they can be divided into enzymatic, immunochemical and non-enzymatic receptor biosensors.

Figure 7: Scheme of a biosensor
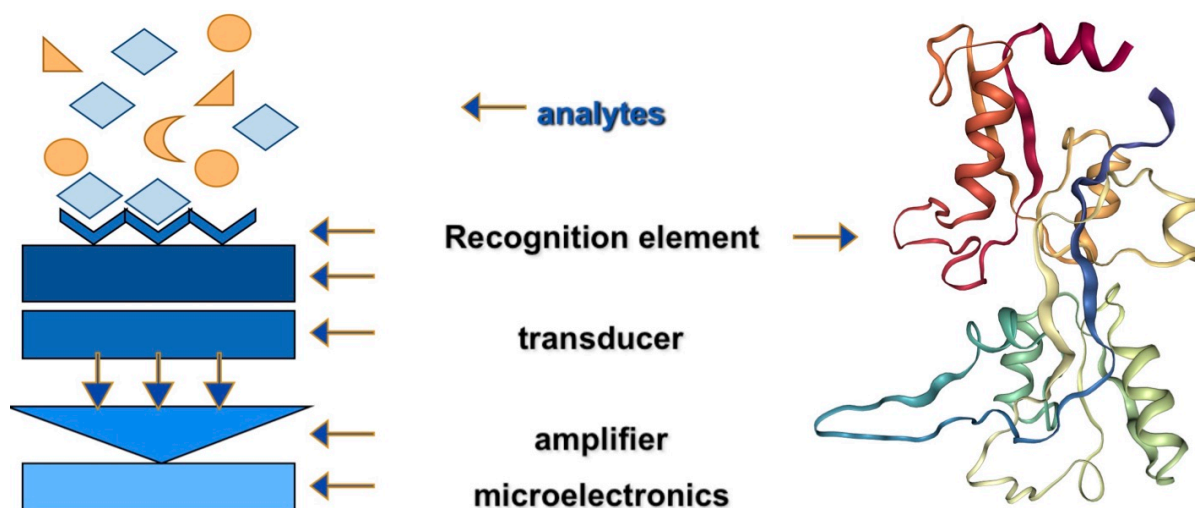
The bio-receptors absolve a crucial role in the biosensor development and they provide specificity and sensitivity to the biosensors. The ligand-binding affinity and specificity of the protein could be manipulated to create a sensor and/or a family of sensors with appropriate dynamic range for the specified application, and little or no interference from spurious analytes. The optimization of ligand-binding affinity and specificity is a process that includes different technologies and approaches that are correlated to the class of bio-receptor used. Some of these methods are based on radical computational re-design or *de novo* design of ligand-binding sites. Proteins and enzymes were among the first recognition elements to be incorporated into biosensors. Acting as biocatalytic elements, enzymes enable the detection of analytes in various ways. Since enzymatic reaction is accompanied by the consumption or production of species such as NADH, CO_2, NH_3, H_2O_2, H^+ or O_2, various transducers easily detect and correlate this species to the substrates. Also the inhibition

or activation of the enzyme could be correlated to the substrate concentration. A major advantage of enzyme-based biosensors is the ability, in some cases, to modify catalytic properties or substrate specificity by genetic engineering. The major limitation is the lack of specificity in differentiating among compounds of similar classes. The use of enzymes as biosensors, however, presents the disadvantage of the substrate consumption, which is a disadvantage in a continuous sensors design or in biotechnology assays. Recently, coenzyme-depleted enzymes (apo-enzymes) as non-consuming substrate sensors are used as bio-receptor in the biosensor development (D'Auria & Lakowicz 2001, D'Auria *et al*. 2000). Apo-enzymes are still able to bind the substrate, but not to transform it. Additionally, the binding of substrates may result in enzymatic conformational changes that can be easily detected by spectroscopy methods, such as fluorescence spectroscopy measurements. SBPs are present in the periplasmic space of mesophilic and thermophilic bacterium. These classes of proteins are widely used as probes for reversible optical sensors of analytes with high social impact. The advantages of using this class of proteins is that genetic engineering gives the possibility to modulate the affinity and selectivity of the protein versus new class of analytes and allow us to greatly expand the range of biochemically relevant analytes that can be measured using protein-based sensors (Staiano *et al*. 2010).

Importance of L-glutamate Biosensor

In the last years, the development of a biosensor for glutamate has become an important challenge to check the levels of extracellular glutamate. This amino acid is involved in many metabolic and biochemical pathways, both as a neurotransmitter and as a central molecule in nitrogen metabolism. The control of the glutamate release is of great interest, because high concentrations of extracellular glutamate are toxic to neurons and may lead damage to the brain. Additionally, glutamate is used as enhancer of flavour in the food. Different studies have demonstrated that high concentrations of this compound in food are toxic for human health (Hamdam & Mohd Zain 2014). Due to the glutamate excitotoxicity, and key rule brain functions, there is a need to develop high sensible methods for glutamate detection. In fact here are several analytical methods used for glutamate detection: magnetic resonance (Wang *et al*. 2012), capillary electrophoresis (Hernandez *et al*. 1993), high performance liquid chromatography (Clarke *et al*. 2007) and micro-dialysis (Qin *et al*. 2013) These techniques have some disadvantages: are invasive, are temporally limited, have low signal-to-noise ratio and they cannot detect changes in glutamate transport under physiological conditions. To overcome these disadvantages, enzymatic biosensors have been used, but they have a relatively low sensitivity, low signal-to-noise ratio and they cannot quantify rapid neurochemical kinetics during synaptic transmission. Electrochemical methods are the most used because they have high

sensitivity, selectivity reproducibility. They are inexpensive, fast and provide accurate results; among electrochemical biosensors, the most used is the amperometric biosensor (Kaivosoja *et al*. 2015). L-glutamate is not electrochemically active and then, for his detection, it is necessary that a glutamate oxidase be used. The glutamate oxidase catalyzes the oxidative deamination of glutamate leading to the formation of hydrogen peroxide. This kind of biosensor is sensitive to pH. In fact, the glutamate oxidase has an optimal activity at pH 7.5 and this fact represents a disadvantage because the enzyme activity can be altered by not optimal pH (Soldatkin *et al*. 2015). A way to detect glutamate is based on the activity of the glutamate transporters and on their ability to maintain low levels of glutamate. In this biosensor the radioactively L-[^{14}C]-glutamate is used. A disadvantage of this approach is due to consumption of the glutamate by glutamate oxidase. This biosensor cannot give an accurate response on levels of glutamate (Kaivosoja *et al*. 2015). A nano-sized fluorescence chemosensor is much used in biosensing for its properties: large surface area, improved mechanical flexibility, thermal resistance property, chemical stability and environmentally friendly nature. Moreover, these biosensors are able to detect low glutamate concentration and so their sensitivity is increased (Soldatkin *et al*. 2015). Although there have been improvements, these biosensors are based on the use of the enzymes and so the detection of the analyte can occur only with a chemical reaction. The need to develop a fast, simple and sensitive glutamate biosensor has resulted in the use of a glutamate-sensitive fluorescent reporter. It was obtained by linear genetic fusion of a glutamate PBP (Gltl) with enhanced cyan fluorescent protein (ECFP, a yellow fluorescent protein). The main limit of this approach is due to a low signal-to-noise ratio that limits quantitative measurements of rapid glutamate transients (Hires *et al*. 2008).

Future Prospective: GluB lipoprotein-FRET Based Biosensor

In recent years, fluorescent protein sensors have been developed based upon the natural affinity and specificity between a protein and its substrate (Coulet & Bardeletti 1991). A schematic model of FRET sensors for metabolites was described in Figure 8 (adapted from Bermejo *et al*. 2011). The recognition element is a cartoon representation of a substrate-binding protein, its ligand (analyte) is depicted as a peanut shape, the short-wavelength fluorophore (SWF) is a blue barrel, the long-wavelength fluorophore (LWF) is a yellow barrel and dark grey bars represent rigid linkers (panel A). Performing an excitation with short-wavelength (e.g. indigo) provides maximal excitation of SWF, and thus high cyan emission intensity, but provides minimal excitation of LWF leading to minimal yellow emission (panel B). In panel C excitation is shown with long wavelength (e.g. green); in this example green excitation provides maximal excitation of LWF, and thus minimal cyan emission intensity. In the upper of panel D is shown the fusion of the SWF and LWF via a

rigid linker when the SWF is excited with indigo light and the fluorophores are in foster distance (1-10 nm), some of the energy is transferred from the SWF to the LWF, resulting in reduced cyan emission and increase yellow emission. In the lower panel: SWF and LWF are coupled to specific amino acid in the N- and C-termini of the substrate-binding protein. In this example in the absence of the analyte, the energy transfer is about 50%. Note that peptide bonds in the linker are rotable. Thus since typically many molecules are analysed over comparatively long time intervals relative to fret, the fluorophores will occupy a wide range of positions, leading to averaging. When the analyte (such as glutamate) binds, conformational changes in SBP occur and can lead to increase energy transfer, as shown in the example here is about 75%. These properties can be used to develop a FRET-based biosensor for glutamate detection. In this context, we studied the possibility to develop a fast, stable and reagentless glutamate biosensor using an SBP. For this purpose, we have chosen the GluBP isolated from *Corynebacterium glutamicum*. We have investigated the effect of the binding of L-glutamate on the structural stability of the recombinant glutamate-binding protein (GluBP/glutamate complex and GluBP alone) by Steady-State Fluorescence techniques and Far-UV CD spectroscopy in thermal scan experiments at different pH of buffer and presence of different cations.

Aim of the work

Cloning, Expression, Purification and Spectroscopic characterization of GluBP a New L-glutamate Molecular Recognition Element isolated from *Corynebacterium glutamicum*

The aim of this work is the cloning, expression, purification and spectroscopic characterization of GluBP, a SBP isolated from *Corynebacterium glutamicum*, a Gram-positive bacterium. This protein is responsible of the uptake of L-glutamate in this bacterium and recently a crystal of GluBP was obtained but has not been resolved by X-Ray crystallography (Liu *et al*. 2013). GluBP is a potential candidate as MRE to detect L-glutamate. L-glutamate, as a neurotransmitter, is involved in different physiological processes. Moreover it is mainly used in food industrial as flavour enhancer in the form of sodium salt. Besides it is essential control glutamate levels in the food and in the human fluid because of its brain excitotoxicity. GluBP is a potential candidate for development of a fluorescent biosensor for L-glutamate and for this reasons it very important obatain its spectroscopic characterizations.

Figure 8: Future application of GluBP /glutamate complex for fluorescent based biosensor adapted from Bermejo _et al._ 2011
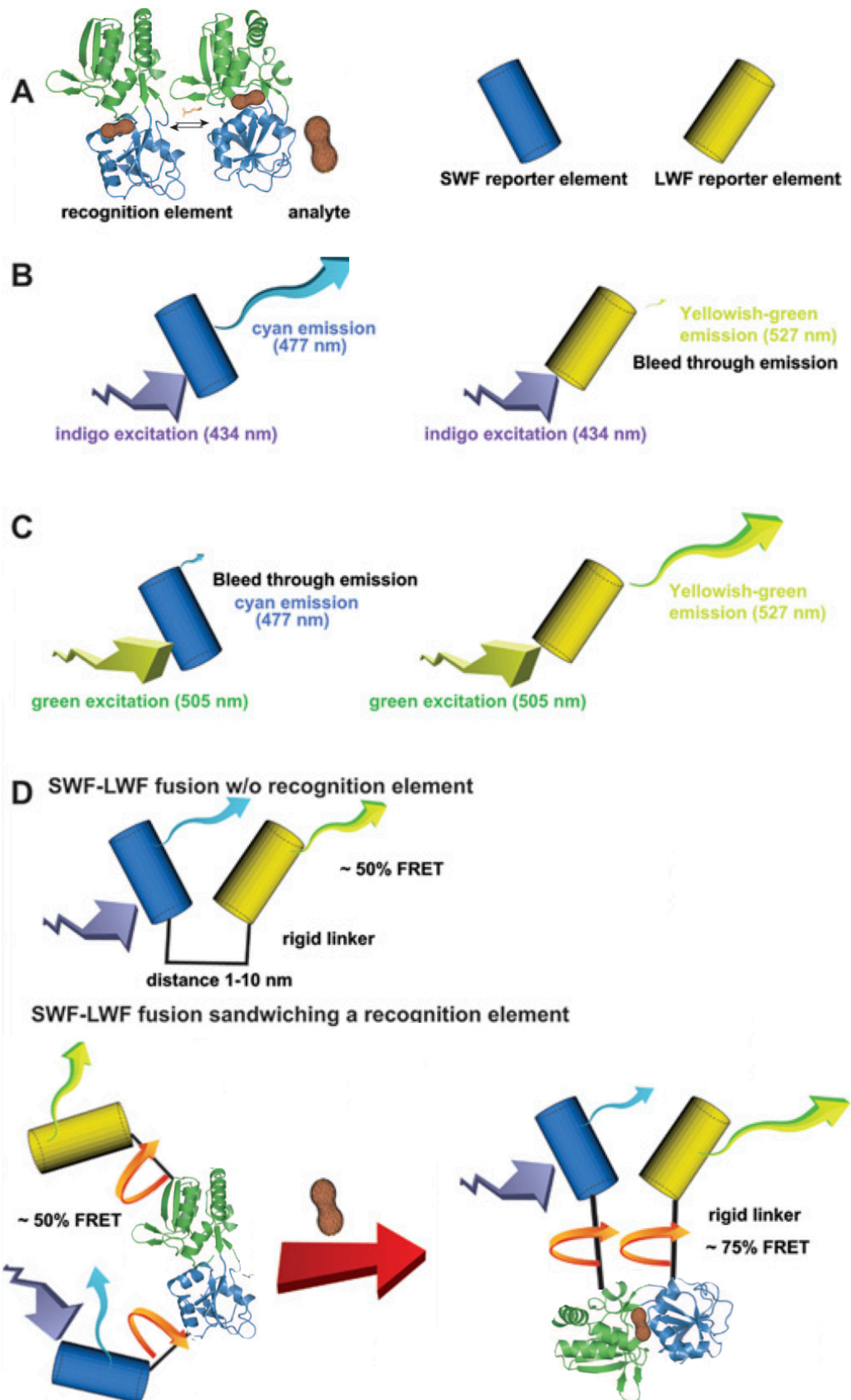
Material and Methods

### Cloning, expression and purification of GluB lipoprotein and His-tag GluBP

The genes encoding full-length (lipoprotein) and the N-truncation fragment (His-Tag protein) of GluB were amplified by PCR cloning from the chromosome DNA of *Corynebacterium glutamicum* res 167 strain using the following primers:

Table 1

Primers name	Restriction Enzyme	Plasmidic Construct	Cloning in pET28a(+) for GluB pre-protein
Forward pgluB_for	(*NdeI*)	**pET28a-gluB**	5'- ggaattc*CATATG*TCTGCAAAGCGTAC -3'
Reverse pgluB_rev	(*EcoRI*)	**pET28a-gluB**	5'- ccg*GAATTC*TTATTAGCTTGCGTCGAGGAAGG -3'
Primers name	Restriction Enzyme	Plasmidic Construct	Cloning in pET22b(+) for GluB mature protein
Forward mgluB_for	(*NdeI*)	**pET22b-gluB**	5'- agctgaCATATGGACGGATTCCTCGCAGCCATTGAAAATG-3'
Reverse mgluB_for	(*NotI*)	**pET22b-gluB**	5'- gacagtGCGGCCGCGCTTGCGTCGAGGAAGGAGAGGTCACC-3'
pET_for		**Colony PCR**	5'- CGATCCCGCGAAAATTAATACG -3'
pET_rev		**Colony PCR**	5'- CAAGACCCGTTTAGAGGCCCC -3'

The DNA sequence gene of pre-GluB, with the signal peptide coded for the N-terminal peptide of 34 aa, was cloned into expression vector pET28a(+) between the NdeI and EcoRI restriction sites. The DNA sequence gene for mature form of GluBP, with the N-terminal 34 residues removed, was cloned into expression vector pET22b(+) between the NdeI and NotI restriction sites and a six-histidine tag was engineered at the C-terminus.

Figure 9: Restriction-map vectors used in cloning of ORF sequence of gluB gene
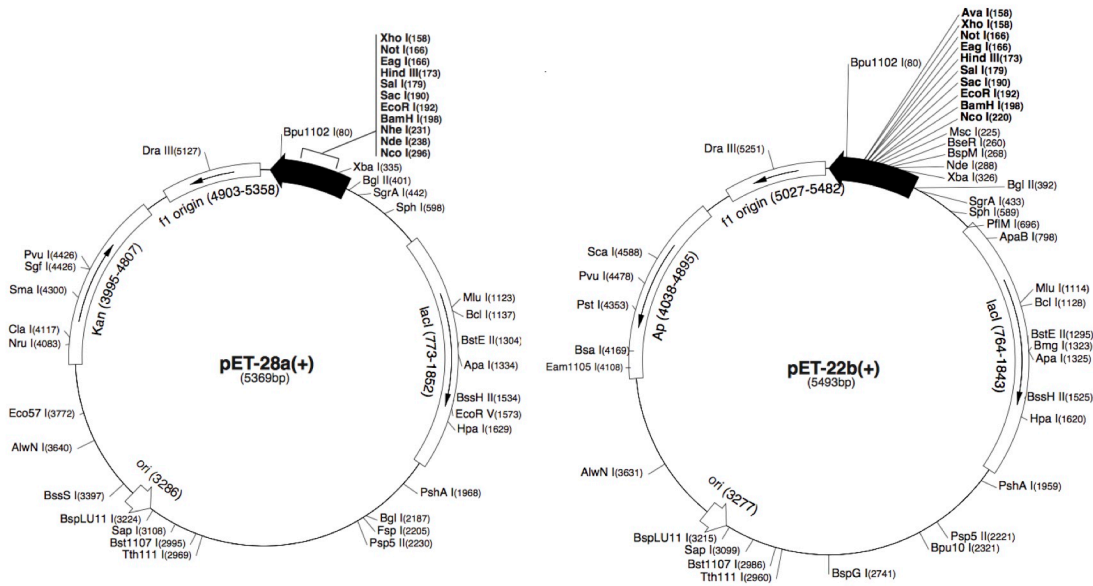
Figure 10: shows the GluBP sequence and processing in pET-22a(+) vector

N-term sequencing (yellow), HIS-Tag (green) and N-palmitoyl Cysteine (pink) have been highlighted. Molecular Weight of GluB lipoprotein is 28.7 KDa.

Molecule processing

Signal peptide 1 – 26	26	By similarity
Chain 27 – 295	269	Glutamate-binding protein
Lipidation 27	1	N-palmitoyl cysteine Probable
Protein sequence 29 – 35	6	N-term sequencing

MGSS HHHHHH SSGLVPRGSH   HIS-TAG

```
        10          20          30          40          50          60
MSAKRTFTRI  GAILGATALA  GVTLTACGDS  SGGDGFLAAI  ENGSVNVGTK  YDQPGLGLRN

        70          80          90         100         110         120
PDNSMSGLDV  DVAEYVVNSI  ADDKGWDHPT  IEWRESPSAQ  RETLIQNGEV  DMIAATYSIN

       130         140         150         160         170         180
AGRSESVNFG  GPYLLTHQAL  LVRQDDDRIE  TLEDLDNGLI  LCSVSGSTPA  QKVKDVLPGV

       190         200         210         220         230         240
QLQEYDTYSS  CVEALSQGNV  DALTTDATIL  FGYSQQYEGD  FRVVEMEKDG  EPFTDEYYGI

       250         260         270         280         290
GLKKDDQEGT  DAINAALERM  YADGTFQRLL  TENLGEDSVV  VEEGTPGDLS  FLDAS
```

The recombinant GluBP contains residues 35-295 of the pre-GluBP sequence, preceded by methionine and followed by AAALEHHHHHH (Liu *et al.* 2013). The recombinant plasmids were obtained by ligation reaction (Thermo Scientific Rapid Ligation Kit) of PCR products (KOD Hot Start DNA Polymerase) and vectors digested with appropriate Restriction Enzyme (See Table 1). Obtained vectors, they were transformed into DH5αMCR^R competent cells. The presence of the mcrA genotypic marker and the deletion of mcrBC and mrr make this strain suitable for cloning DNA containing methylcytosine and methyladenosine (Raleigh *et al.* 1988). Therefore, genomic DNA, both prokaryotic and eukaryotic, can be cloned efficiently in DH5αMCR (Raleigh *et al.* 1988). Finally, the selection on LB + kanamycin 50 µg/ml or 100 µg/ml ampicillin was performed. Colony PCR screenings (See Table 1) were performed and plasmid preparation of two positive clones (Qiagen Plasmid Plus midi Kit) were both digested with restriction enzymes XhoI and PvuI. DNA sequences of two positive clones were performed and one clone for each different cloning procedure was transformed into *Escherichia coli* strain BL21 (DE3). The bacteria were grown in pre-culture plus 1% glucose and main culture LB medium with kanamycin (25 µg/ml) and ampicillin (100 µg/ml), with transformed BL21(DE3) cells, pET28a(+) and ET22b(+) respectively, until reaching an optical density (OD) of 0.6 at 600 nm. So, the induction tests were performed (See Figure 13A) to determine the optimal conditions for GluBP expression. Preliminary, experiments have shown that a good protein expression was obtained by 0.2 mM isopropyl β-D-1-thiogalactopyranoside (IPTG). To determine the optimum induction time and temperature, we have carried out three bacterial growths simultaneously. In one of three growths, we induced with 0.2 mM IPTG at 22 °C, in another with 0.2 mM IPTG at 25 °C and in the last one with 0.2 mM IPTG at 18 °C. All three of the growths were carried out up to overnight. The GluBP expression was monitored at hourly intervals for 4 hours and finally ON. The cells were harvested by centrifugation at 4000 rpm at 4 °C for 20 minutes. The cells were suspended in lysis buffer (50 mM NaH$_2$PO$_4$/Na$_2$HPO$_4$$^{3-}$, 300 mM NaCl, pH 8.0) and lysozyme (0.4%), DNase (0.05 γ/λ) and MgCl$_2$ (5 mM) were added and incubated for 1h at room temperature (RT). The cells re-suspended were lysed using French Press (3 cycles). The lysate was centrifuged at 3000 rpm at 4 °C for 20 minutes. The supernatant (lysate) was filtered by a filter with a KO of 0.22 µm, the seven ml of lysate obtained from Hit-Tag construct was loaded onto 2 ml of Ni-Nta Resin (Qiagen) and left in agitation for two hours at 4 °C. The flow-through was collected after e the incubation of 30 min at RT in a collection tube. The column was washed performing three wash volumes (pre-wash) of lysis Buffer (50 mM NaH$_2$PO$_4$/Na$_2$HPO$_4$$^{3-}$ pH 8.0, 300 mM NaCl). The proteins were eluted by doing three elution volumes with increasing concentration of imidazole (respectively 0, 10, 20, 50, 100 and 250 mM imidazole).

Sodium Dodecyl Sulfate-PolyAcrylamide Gel Electrophoresis (SDS-PAGE)

The SDS-PAGE analyses have been used extensively to assess protein purity and carried out according to Laemmli method (Laemmli 1970). Gels were 0.75 mm thick and consisted of an upper stacking gel and a lower resolving gel, respectively of 4% and 15% polyacrylamide, containing 0.1% SDS, and a buffering agent (Tris/HCl). The running buffer, in which the gels bathe, had the following composition: 25 mM Tris (pH 8.3), 250 mM glycine and 0.1% SDS. Laemmli buffer was added to the samples and were boiled at 98 °C for 10 minutes. The samples were then centrifuged at 13000 g for 10 second and loaded into the corresponding well. Then the electrophoresis was carried out at 100 Volts constant in SDS running-buffer (Tris 0.125 M, glycine 0.96 M, SDS 0.5%). As a standard it was used the Amersham Low Molecular Weight Calibration Kit for SDS Electrophoresis (GE Healthcare).

Figure 11: Ni-Nta Sepharose performed on Bl21 (DE3)/pET22b-gluB lysate (A) and Spin Column Ni-Nta on Bl21(DE3)/pET28a-gluB lysate (B) of Affinity Chromatography SDS-PAGE
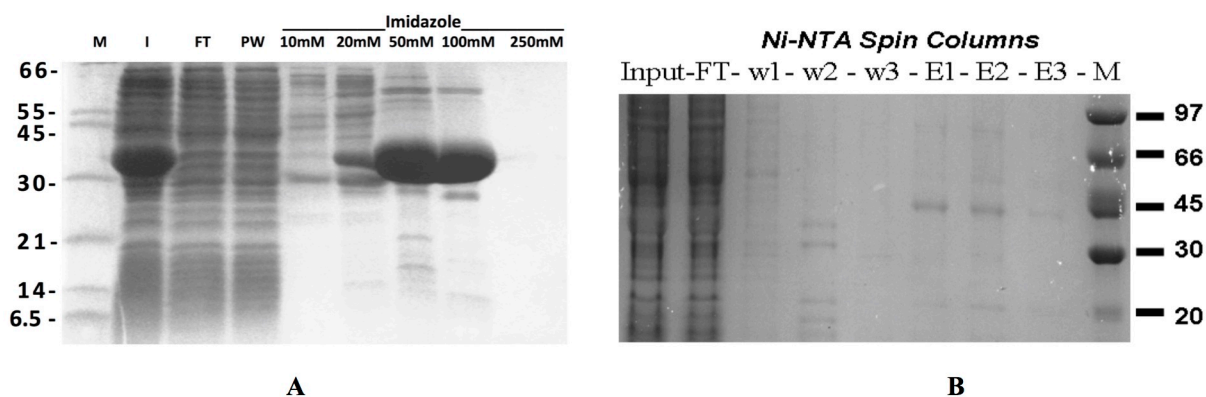
Native-PolyAcrylamide Gel Electrophoresis (Native-PAGE)

The native PAGE analyses have been used extensively to assess protein purity and carried out according to modified Laemmli method. Gels were 0.75 mm thick and consisted of an upper stacking gel and a lower resolving gel, respectively of 4% and 15% polyacrylamide, without SDS, and a buffering agent (Tris/HCl). The running buffer, in which the gels bathe, had the following composition: 25 mM Tris (pH 8.3), 250 mM glycine. Laemmli buffer without SDS in presence of buffer Tris pH 10 was added to the samples and did not boiled at 98 °C for 10 minutes. The samples were then centrifuged at 13000 g for 10 second and loaded into the corresponding well. Then, the electrophoresis was carried out at 100 Volts constant in running Buffer (Tris 0.125 M, glycine 0.96 M) for 3 hours. As a standard, it was used the Amersham Low Molecular Weight Calibration Kit

for SDS Electrophoresis (GE Healthcare) samples of this LMW were diluted in the same modified Laemmli (without SDS at pH 10) and incubated for 20 minutes at RT. Inside low molecular protein marker, it was present a protein Ovalbumin from chicken eggs (OVA) that has isoelectric point at pH 4.5 very close to GluBP (PI= pH 4.2) (See Figure 26B). This protein was taken as reference molecular weight of 45 KDa in native PAGE experiment.

Gel Filtration of GluBP at pH 8.3 in the presence of increasing concentration of NaCl

Relative motilities of 1.5 mg GluBP diluted in 500 μL of 20 mM buffer sodium phosphate buffer (pH 8) in the absence and in the presence of salts (NaCl) were determined by size-exclusion chromatography (SEC) using a Superdex 200 10/300 GL column (Amersham) equilibrated in each experiment with 50 mM Tris-HCl (pH 8.3) and 0, 0,15 and 0,5 M NaCl respectively, at a flow rate of 0.5 ml/min. Chromatograms of three different experiments were shown in Figure 26A.

Western blot Experiments and N-terminal edman sequencing of GluB lipoprotein

The proteins, contained in different fractions of IEC or immunoaffinity cromatography, were loaded, separated by sodium dodecyl sulfate-polyacrylamide gel electrophoresis (15% SDS-PAGE), and then transferred overnight at 4 °C to PVDF membrane (Millipore) using the Trans-Blot Semi-dry System (Biorad Laboratories). The membrane was blocked for 2 hours at RT by using 5% non-fat dry milk in phosphate buffered saline. After three washings with PBS-Tween (PBS-Tween 0.05% 10 minutes per washing), the membranes was probed for 2 hours at RT with the following antibody directed against produced His-Tagged proteins: anti-polyHistidine-Peroxidase clone HIS-1 mouse monoclonal (Sigma) dissolved in PBS-Tween 0.05% /1% bovine serum albumin. Finally, the filter was washed three times as described above and bands were detected by peroxidase chemiluminescence (ECL). For N-term sequencing of eluted protein from DEAE cromatography, 15% SDS-PAGE of many samples was electroblotted for an hour at RT to PVDF membrane in tranfer CAPS buffer 10 mM CAPS (3-cyclohexylaamino-1-propane sulfonic acid) adjusted with NaOH (2N) to pH 11/10% MeOH, PVDF membrane was washed extensively with milliQ water, stained in Ponceau S (freshly prepared 1% Ponceau S/ 10% acetic acid for two minutes) and destained in milliQ water (Millipore). Only Ponceau solution with 10% acetic acid stained GluBP since very low isoelectric point (IP) of protein pH 4.2. Finally the protein bands of apparent molecular weigth of 37 KDa analysed by N-terminal Edman sequencing. In below figures, the obtained sequence was highlighted in yellow.

Glutamate-binding protein: sample quantization

Before starting spectroscopy experiments, it is essential to remove any glutamate bound to the protein following purification. For this purpose, we performed an extensive dialysis of the isolated protein against Phosphate Buffered Saline (NaPO$_4^{3-}$ or KPO$_4^{3-}$) at pH 8 and pH 7. In particular, the sample was dialyzed for two days using a dialysis membrane with cut-off 3000 Da and a solution of 50mM NaPO$_4^{3-}$ at pH8 and 300 mM NaCl (two change of buffer/day) ad after another day to final pH (two change of buffer/day). The purity and the concentration of the protein were evaluated by analysing SDS-PAGE and the absorption spectra. The sample was analysed in a range of wavelengths between 220 and 320 nm. Spectra were recorded on a Cary 50 Bio UV/Vis spectrophotometer (Varian) data not shown. The protein concentration was calculated on the basis of the absorbance values at 280 nm by, using the Lambert and Beer's law. The sequence of GluBP includes two tryptophans (W), eleven tyrosines (Y) and three cysteines (C) residues and its calculated molar extinction coefficient is $\varepsilon_{molar} = 27640 M^{-1} cm^{-1}$ and percent extinction coefficient of $\varepsilon_{Percent}$ of 8.6 were calculated by these formula (Pace *et al.* 1995):

$$i) \ \varepsilon_{molar} = \big((nW \times 5500) + (nY \times 1490) + (nC \times 125)\big)$$

$$ii) \ \Big(\varepsilon_{percent}\big(^g/_{100 \ ml} = 10 \, ^{mg}/_{ml}\big)^{-1} cm^{-1}\Big)$$

$$iii) \ (\varepsilon_{molar}) M^{-1} cm^{-1} \times 10 = (\varepsilon_{percent}) \times \big(10 \, ^{mg}/_{ml}\big)^{-1} cm^{-1} \times (Mw) Da$$

e.g. : for a calculated molecular weight of Globe about 32 KDa a solution of GluBP that absorbs 0.1 OD$_{280}$ has a concentration of 0.11 mg/ml.

Circular Dichroism measurements

Measurements were performed on homogeneous samples of GluBP in 20 mM sodium or potassium phosphate pH 8.0 or pH 7.0, with a protein concentration of 6.3 μM and specified 100 μM of L-glutamate. Measurements with other aminoacids were performed with different ratio aminoacid/protein for testing specificity of GluBP for L-glutamate. Protein concentration were reduced by 1/5 (12.5 μM), concentration of aminoacids was not modified (100 μM) (L-glutamate L-glutamine and L-aspartic) in range concentrations that no optical activity were observed (data not shown). Results were showed in Figure 18.

Far-UV CD analysis was performed on a Jasco J-810 CD spectrometer (Jasco, Tokyo, Japan) equipped with temperature-controlled liquid system (Julabo F25 MA Seelbach, Germany). The

instrument was calibrated by a standard solution of (+)-10- camphor sulfonic acid. Sealed cuvettes with a 0.1 cm, path length (Helma, Jamaica, NJ) was used with a photomultiplier voltage never exceeding 600 V in the spectral regions measured with 0.1 nm step size. The spectra were recorded over wavelength range 190-260 nm in a 1mm cell at sample concentration of 0.2 mg/ml at 20 °C. The samples volume required for analysis was 0.4 ml. The final spectra were the average of five scans, and the analysis took about 15 minutes for all the scans for each temperature.

Each spectrum was averaged five times and smoothed with Spectropolarimeter System software (Jasco, Japan). All measurements were performed under nitrogen flow. Before undergoing CD analyses, all samples, after an hour of incubation at RT, were kept at the temperature to be studied for ten mins (D'Auria *et al*. 1996). Protein absorption spectra were recorded before and after collecting CD spectra. CD spectra of the buffer solution in the appropriated cuvette were subtracted from the sample spectra and smoothed using the Savistky-Golay function. The results are expressed in terms of molar ellipticity (θ).

Steady-State Fluorescence Spectroscopy

Steady state emission experiments were done on an ISS-K2 fluorometer (ISS, Urbana-Champaign) with excitation wavelength of 295 nm. These experiments were carried out in order to remove the effects of tyrosine residues, resulting from fluorescence spectra and monitoring emission of Trp that is influenced by local microenvironment. The emission slit width was of 1 nm and the emission spectrum recorded from 310 and 410 nm. Samples were placed in the thermostatic holder and temperature of samples was measured directly in the cuvette with an accuracy of ± 0.2 °C. in a double holder and continuously monitored at each measurements.

The pH effect was studied in the range 6.0- 8.0 after overnight incubation at 4 °C. The Steady-State Fluorescence measurements at different pH were carried out in 20 mM Na phosphate buffer (pH 6.0- 8.0). All the solutions were prepared in distilled water and GluBP samples at different pH values were prepared by dissolving the protein at the final concentration of 17.2 μM, by diluting a stock solution of 64.5 μM stored at 4 °C in a lysis buffer 300 mM NaCl 50 mM $NaPo_4^{3-}$.

Glutamate Titration of GluB lipoprotein

The glutamate/GluBP interactions were studied by a fluorescence titration approach. The binding of glutamate to GluBP was estimated by a variation of the intrinsic protein fluorescence tryptophan (W) emission in two distinct experiments. For this purpose, recombinant GluBP was titrated by increasing concentrations of glutamate (0- 3 mM) and keeping it in constant stirring. Experimental data were processed by a non-linear regression analysis for best fitting curves computed with the

Origin pro. In the first experiment different, samples of GluBP (11 μM) were incubated with increasing concentration of glutamate in incubation over night at 4 °C. In the second experiment, 2 μL of increasing glutamate concentration was added sequentially to protein dissolved in buffer and was performed an incubation of 15 mins at RT, before collecting spectra sequentially. Spectra were corrected by adding a diluted solution glutamate. In either experiments, the data showed were the media of three spectra obtained by scan step of 2 nm/sec. The maximal decrease of the protein fluorescence, due to the saturation of the binding sites by the ligand (F_{max}), was estimated from the titration data. All measurements were carried out using GluBP dissolved in 20 mM phosphate buffer at pH 7. The Steady-State Fluorescence data were performed on a K2 spectrofluorometer. Apparent binding constants were calculated from the titration data using below equation (Dattelbaum & Lakowicz 2001):

Equation 1

$$\Delta F = \Delta F_{max} \left(1 + \frac{K_D}{S} \right)$$

Where ΔF is the change in fluorescence emission, ΔF_{max} is the change in fluorescence in the presence of saturating amounts of glutamate (about 3 mM), S is the concentration of glutamate, and K_D is the apparent binding constant.

Fluorescence Quenching

Steady state emission experiments were done on an ISS-K2 fluorometer (ISS, Urbana-Champaign) with excitation wavelength of 295 nm and the emission slit width of 1 nm. Samples were placed in the thermostatic double holder (for constant monitoring temperature). Acrylamide quenching of the Trp fluorescence was observed at fluorescence maximum. All fluorescence experiments were done in appropriate sodium phosphate buffer, at different pH, with the protein concentration of 0.55 mg/ml to perform experiment (with or without 100 μM L-glutamate) with absorption to 295 nm of 0.1 OD. All fluorescence experiments were done in the 20 mM sodium phosphate buffer, pH 8 with the protein concentration of 11 μM.

8-anilino-1-naphthalenesulfonic acid (ANS) binding experiments in the absence and in the presence of L-glutamate

The ANS is an extrinsic fluorescence probe that binds to the hydrophobic cluster of protein (Paul *et al.* 2008). The fluorescence spectra of ANS (50 μM) were investigated upon incubation with GluBP (17.2 μM) at different pH 10 min (Busby *et al.* 1981; Wicker *et al.* 1986; Ding *et al.* 2010; Wang *et*

al. 2012). The ANS fluorescence spectra were recorded in the range of 400–600 nm with λex = 380 nm (Wang *et al.* 2012; Zhang *et al.* 2011). The ANS experiments were performed on GluBP samples at pH 2.0, pH 8.0 and pH 11.0. GluBP was diluted with buffer at different pH, the final concentration of GluBP was 17.2 µM. An amount of the ANS was added, such that the number of moles of the ANS was tenfold greater than the mole of the protein. The excitation λ of 370 nm, that is the wavelength of absorption of ANS, was used. Overnight incubation with L-glutamate of 100 µM was performed at 4 °C, all measurements were performed at RT after 30 mins of incubation and only after that the ANS was added.

Results and Discussion

gluB cloning in pET22a(+) and pET22b(+) vectors with or w/o His-Tag C-Term

The gene of GluBP was isolated from *Corynebacterium glutamicum*. The gene *gluB* was cloned into expression vectors pET22a(+) and pET22b(+). In the former, vector (pET22a(+)) was cloned by sequence of gluB coding for a pre-protein with signal peptide. In lysate obtained by *E. coli* BL21(DE3), this sequence was recognized by peptidase machinery as in *C. glutamicum* (Liu *et al*. 2013) in order to obtain a mature form of GluB lipoprotein, as it was possible to observe in Western blot experiment with antibodies against His-Tag. In WB experiment, antibodies against His-Tag did not recognize GluBP eluted by DEAE Sepharose but only a protein at higher molecular weight (42 KDa) purified and concentrated by spin column Ni-Nta. In this experiment, all proteins visible on PVDF membrane by Ponceau staining were processed in a protein at expected lower molecular weight about 32 KDa and apparent molecular weight of 37 KDa, as it is possible to obtain by mature form of GluBP and by peptidase cutting also in *C. glutamicum*. In the latter, vector a sequence lacking of N-term signal was cloned, and it is possible to obtain a mature form (without any processing) fused at C-Term with His-Tag (6 histidines) useful for Ni-Nta affinity chromatography (Qiagen). Primers, used for cloning and production of pre-protein and mature form of GluBP, were shown in the Table 1. By using these two cloning strategies, it was possible to obtain a mature form of GluBP and to demonstrate if processing by peptidase and probable palmitoylation resulted important for L-glutamate binding of GluBP.

Cell growing and expression in E. coli BL21(DE3) of lipoprotein or His-Tag protein

The gene gluB into the expression vectors pET22b(+) and pET22a(+) was expressed in *E. coli* BL21(DE3). The *E. coli* BL21(DE3) competent cells are widely used for a high level of protein expression and easy induction. They have been specifically constructed for high-level expression of recombinant protein, thanks to their two important features: key genetic markers and inducibility of protein expression. The genetic markers allow to the proteins to accumulate at high levels without degradation while the easy induction permit to minimize the toxic effects of some recombinant proteins. Furthermore, this strain has shown to achieve high levels of protein expression in T7 RNA-polymerase based system that minimizes the level of basal expression, which could decrease rate of duplication of bacteria. The transformation of BL21(DE3) cells with the appropriate vectors cloned with *gluB* gene, were carried out. The colonies obtained from these transformations were used for bacterial growth following the protocol described above. The optimal condition of GluBP expression was found. The transformed BL21(DE3) cells were grown until reaching an optical density of 0.6 OD_{600}. We controlled growth progress by OD_{600} measurements each hour for 6 hours

and ON (data not shown). When the cell reached a value of 0.6 OD_{600}, was added IPTG to induce over-expressed protein at optimum conditions. The optimum expression of the proteins was tested, in the temperature range of 18- 24 °C was determined the induction time needed to obtain an optimal expression. At the end of the post-induction incubation, SDS-PAGE at 15% of acrylamide was made in order to evaluate expression levels of GluBP. From the analysis of the results we identify that optimal level of expression of GluBP was obtained following an overnight induction at 22 °C with 0.2 mM IPTG. In Figure 12 it was reported the results obtained by GluB His-Tagged protein but similar results were observed also with GluB lipoprotein but a 30% of this protein (Data not shown) is bound in the pellet and is it possible to wash pellet with lysis buffer (QIAGEN) and to obtain another amount of soluble GluBP, as suggested hypothesis that protein is expressed as lipoprotein in *E. coli* and slowly bound to membrane by lipid anchor. In SDS-PAGE (at expected molecular weight about 32 KDa) No N-term His-Tagged protein was found and visible in pellet obtained after production of this lysate, with the same destruction procedure. Figure 9 reports: the restriction vector maps of pET22b(+) and pET22a(+), and table 1 the different primers used for the two cloning strategies and highlighted N-term sequencing of GluBP purified by Ni-Nta sepharose resin.

A   B
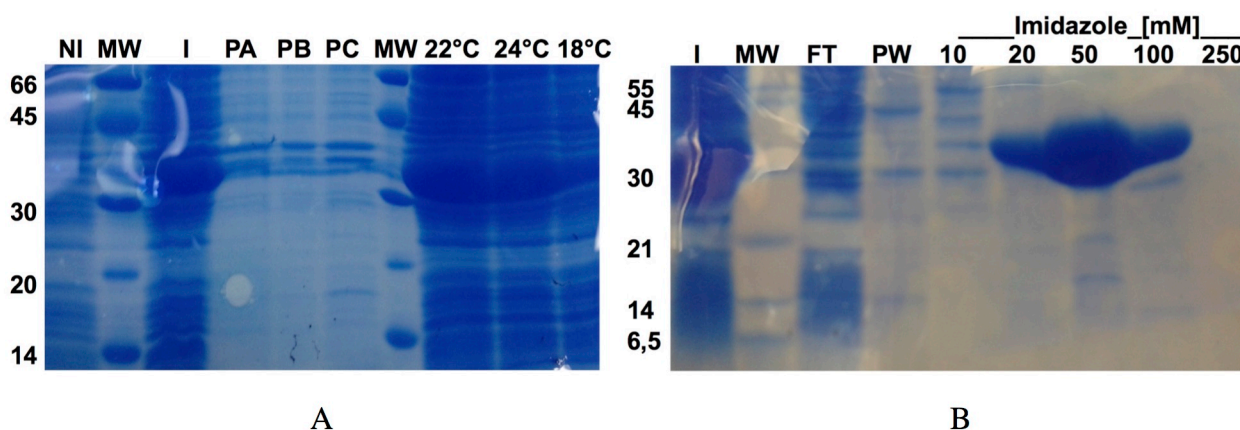
Figure 13: SDS-PAGE
Tests at different temperature of induction of GluBP (A); IN: GluBP induced 3 hours NI: Non-Induced; PA (22 °C), PB (25 °C) and PC (18 °C): pellets of lysate after French Press; 22 °C, 24 °C and 18 °C: Lysate obtained after ON induction with IPTG. B) SDS-PAGE of 2nd Ni-Nta Sepharose Affinity Chromatography.

GluBP purification by DEAE and affinity chromatography and N-term sequencing

Once the cells are induced to express the protein GluB, they are separated from the culture medium by centrifugation. To get only GluBP, it is necessary to apply techniques of purification of the lysate, obtained by breaking cell. For this aim, two different cloning were performed: former the DNA sequence of gluB containing sequence coding signal peptide were cloned in pET22a(+) vector, for subsequently peptidase processing and GluBP probable cysteine palmoitolation, as indicated by N-term sequencing, to obtain a mature lipoprotein (See Figure 14); latter the DNA sequence of mature forms was cloned in pET22b(+) vector containing a sequence coding for His-Tag (six histidines) at C-terminus residues for production of recombinant proteins. The results were the expression of recombinant GluBP with or without a 6x His-Tag fused to its C-terminus. Recombinant lipoproteins can be purified by IEC by using DEAE agorose resin that is possible performs since GluBP has very low IP calculated = pH 4.20. Recombinant proteins containing a 6x His-Tag can be purified by nickel-nitrilotriacetic acid (Ni-Nta) chromatography, which is based on the interaction between a transition Ni^{2+} ion immobilized on a matrix and the histidine side chains. The nitrilotriacetic is used to immobilize nickel to a solid support, because it has four chelating sites for nickel ions. The use of histidine comes from the ability of this amino acid to create strong interactions with the immobilized metal on ion matrices, as electron donor groups on the histidine imidazole ring at pH 8, easy to form coordination bonds with the immobilized transition metal (Bornhorst & Falke 2000). Moreover the six histidines do not perturb the protein function as demonstrated by increasing thermal stability of GluB lipoprotein and His-Tag GluBP by CD and Steady-State Fluorescent experiment as discuss in next section. In Figure 11A and 13B were shown the SDS-PAGEs of the fraction obtained from two affinity chromatographies sequentially performed; and Figure 14A Western Blot with anti His-Tag on lysate (See Figure 14B, for SDS-PAGE after electroblot) by which eluted fractions of DEAE Chromatography were obtained (Figure 14C). So it is possible to monitor processing by peptidase II (Liu. *et al*. 2013) as it is possible observe in image of WB experiment. In His-Tag affinity chromatography (see Figure 13A and B) the presence of the single biggest protein band of the expected molecular weight about 32 KDa and an apparent molecular weight about 37 KDa indicates that the protein was successfully purified by this affinity chromatography. The concentration of GluBP, obtained from this purification, was determined with a spectrophotometer and its calculated molar extinction coefficient. Final concentration of GluBP was determined by Lambert-Beer's law using ε_{molar} of $27640\ M^{-1}\ cm^{-1}$. The calculated value of concentration was 62.5 μM for 10 ml of protein obtained from His-Tagged protein, 9.4 μM for 5 ml of lipoprotein obtained from DEAE chromatography (from about 3 g of each wet pellet).

Western Blot as tool for monitoring processing of GluB lipoprotein and N-term sequencing

It is possible to observe in Western Blot experiment, only proteins obtained by a purification procedure on spin column Ni-Nta (Qiagen) that reduce dilution of eluted protein samples during purification procedure, have an apparent molecular weight about 42 KDa. Antibodies against His-Tag recognized this protein band. The same band is shown in input lysate and did not appear in other lane with protein eluted by DEAE agarose resin. These protein samples during IEC loading lysate on resin were washed out. After purified protein a N-term sequencing of protein immobilized on slice of PVDF membrane was performed. The N-term sequence obtained was the sequence of mature GluB lipoprotein. This protein sequence lack of His-Tag that was removed after protelitic processing. it has been difficul to obtain sequence since part of pool of protein does not chemically react with autotomatic sequencing machinary at the same cycle. Howewer, it was suppose that it was a conseguence of post translational palmoitalotion occured by of N-term cysteyn since sequence obtained has a of mature form of GluBP. A large amount of this protein in the absence of NaCl precipitated and for this reason only few thermal scan experiments of CD and Steady-State Fluorescent were performed to understand stability of this protein in the presence of glutamate at different pH.
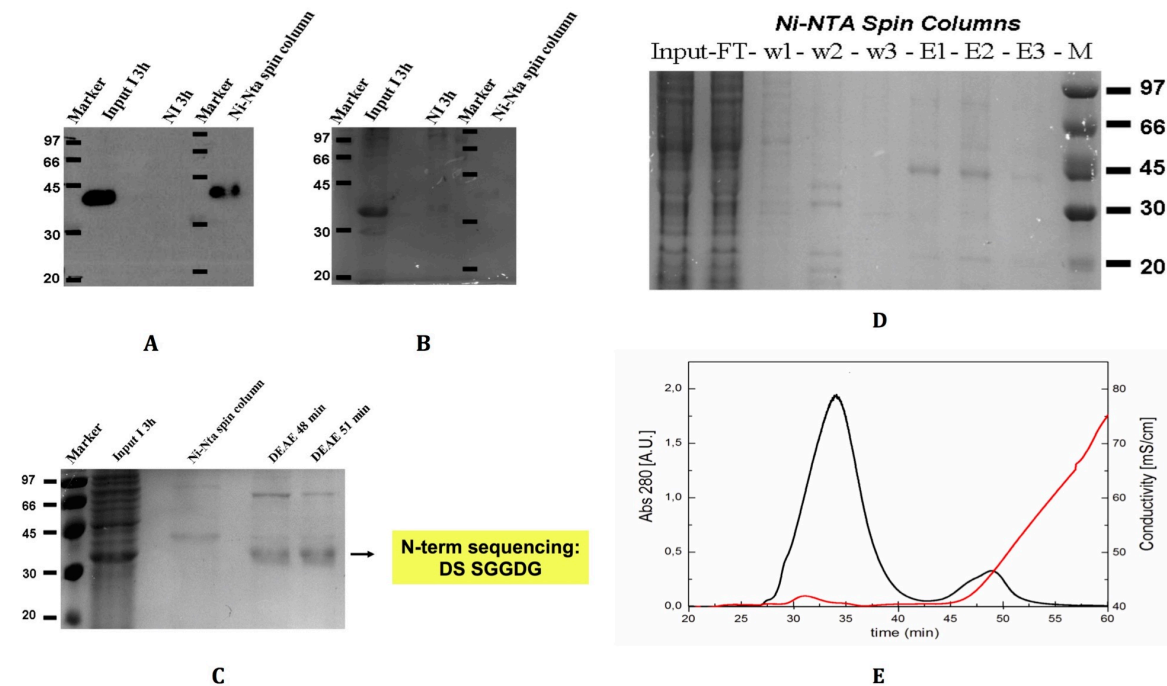
Figure 14: GluB lipoprotein processing
Western Blot experiment on lysate of induced GluB lipoprotein (Input 3 hours) and non-induced (NI 3h), Ni-Nta spin column eluted fraction (A); SDS-PAGE post elettroblotting (B); SDS-PAGE of Ni-Nta/ DEAE eluted samples and highlighted sequence obtained by N-term sequencing in yellow (C); SDS-PAGE of Ni-Nta spin column purification (D); chromatogram of Ion Exchange Chormathography (DEAE) by increasing concentration of NaCl (E).

Circular Dichroism Spectroscopy

The secondary structure content of GluBP in the absence and in the presence of glutamate was evaluated by the Far-UV results. To investigate the effect of glutamate on secondary structure of GluBP, CD experiments in the Far-UV region at RT were performed. The GluBP and Lipoprotein spectra show at low temperature (24 °C) bands characteristic of the α/β protein heating causes progressive unfolding of the protein, the α-helical bands and β-sheet are lost and the bands characteristic of random or disordered structure appear. All proteins spectra show an intense negative band from 208 to 222 nm and a strong positive band about 190 nm. The intensities of these bands reflect α-helical content. Regular all-β proteins usually have a single negative band (210–225 nm) and a stronger positive band (190–200 nm). Intensities are significantly lower than for all-α proteins. Instead as described below, unordered peptides and denatured proteins have a strong negative band (195–200 nm) and a much weaker band (either negative or positive) between 215 and 230 nm. α/β and $\alpha + \beta$ proteins generally have spectra dominated by the α-helical component and, therefore, often show bands at 222, 208, and 190–195 nm. In some cases, there may be a single broad minimum between 210 and 220 nm because of overlapping $\alpha -$ helical and β-sheet contributions. Intensities depend on the α-helical content. As discussed in next section data obtained by CD experiment together to Fluorescent (W) thermal scanning suggest a two-step model of conversion of GluBP structure in two form in stoichiometry equilibrium among them, as indicated by isosbestic point at 206 nm in all experiments performed with GluB lipoprotein-protein/complex at any pH analysed in any buffer used. CD spectroscopy, fluorescence spectroscopy assess the state of folding/unfolding of the protein and thereby can be used to monitor structural change that also might lead to aggregation (Varsha *et al.* 2014 and Berkowitz *et al.* 2012) or formation of dimers, trimers and so on.

GluBP and lipoprotein in (K$^+$) phosphate buffer at pH 7 and relative lower Stability than dialized in (Na$^+$) phosphate at pH 7

Far-UV spectra of GluB lipoprotein in the absence and in the presence of 100 μM glutamate at RT in buffer potassium phosphate was obtained by dialyzed protein in lysis buffer against 20 mM potassium phosphate buffer at 4 °C. GluBP and lipoprotein at low temperature (25 °C) the spectrum shows bands characteristic of the α/β protein heating causes progressive unfolding of the protein, the α-helical bands are lost and the bands characteristic of random or disordered structure appear. All proteins spectra show an intense negative band from 208 nm and a slightly negative band to 218 nm and a strong positive band about 190 nm. The intensities of these bands reflect α-helical content. Intensities depend on the α-helical content. During preparation of this experiment a large amount of total proteins were lost as a consequence of formation of insoluble aggregate. Also

conformational structures are very different to GluBP diluted in buffer sodium phosphate. The loss of negative band at 218 nm at 25 °C and quickly reversible formation of unordered peptides in the range of temperature from 25 to 29 °C with a strong negative band (195–200 nm) and a much weaker band (either negative or positive) between 215 and 230 nm suggests that this protein has less ordered structure than in sodium phosphate buffer.

GluBP and lipoprotein /glutamate complex at low temperature (25 °C) at pH 7 and lipoprotein /glutamate complex at low tempearture (25 °C) at pH 7

As it shown in next section GluBP in the absence of glutamate at 25 °C but in presence of 20 mM sodium phosphate has un ordered structured and higher content of α-helical and β-sheet than in presence of potassium phosphate. For this reason any other experiment was performed in sodium phosphate buffer except that for preliminary titration curve with L-glutamate and thermal scan experiment for understand stability of GluBP and lipoprotein.
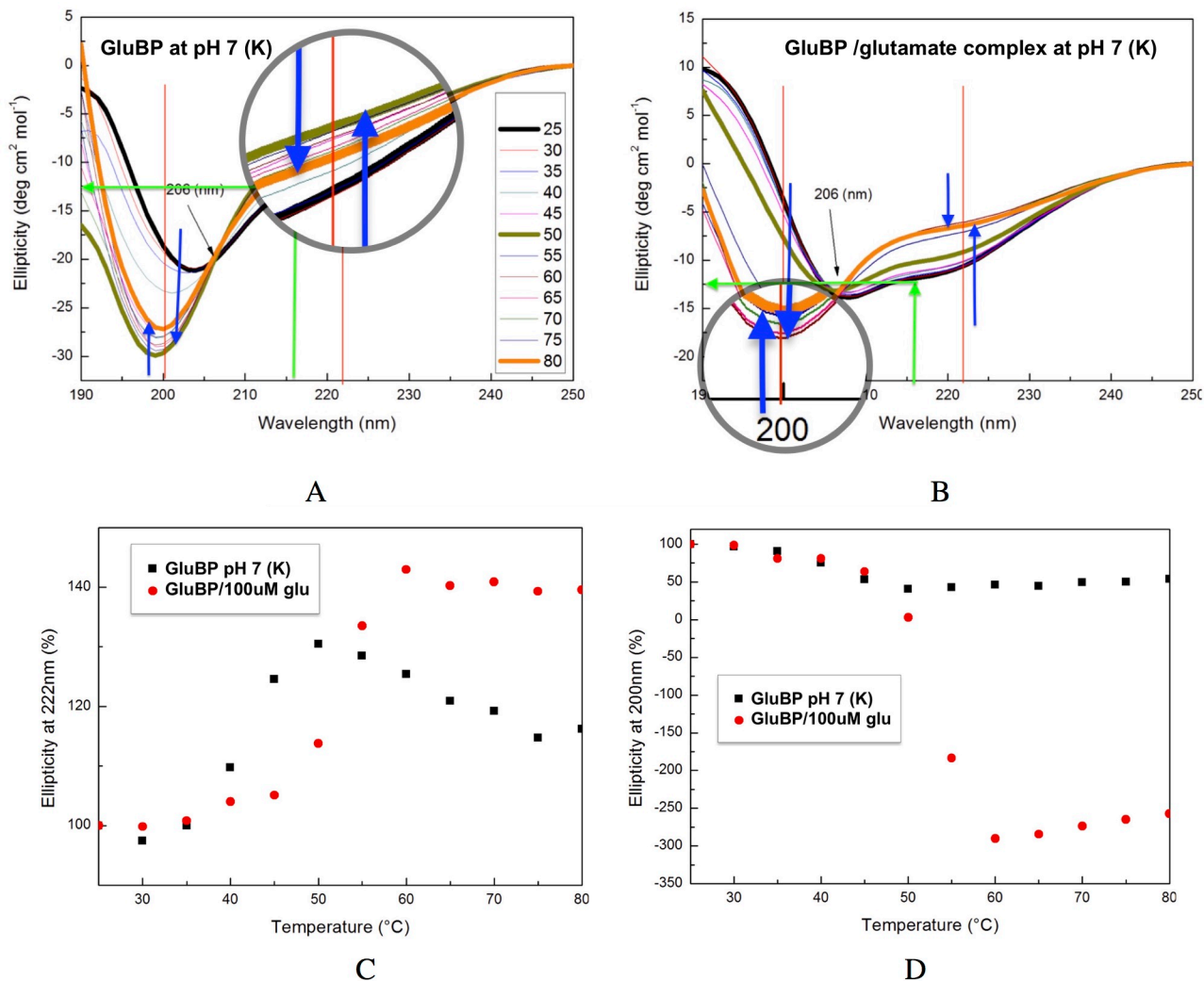
Figure 15: CD Spectra of GluBP/glutamate complex in the presence of 20 mM (K⁺) phosphate buffer at pH 7
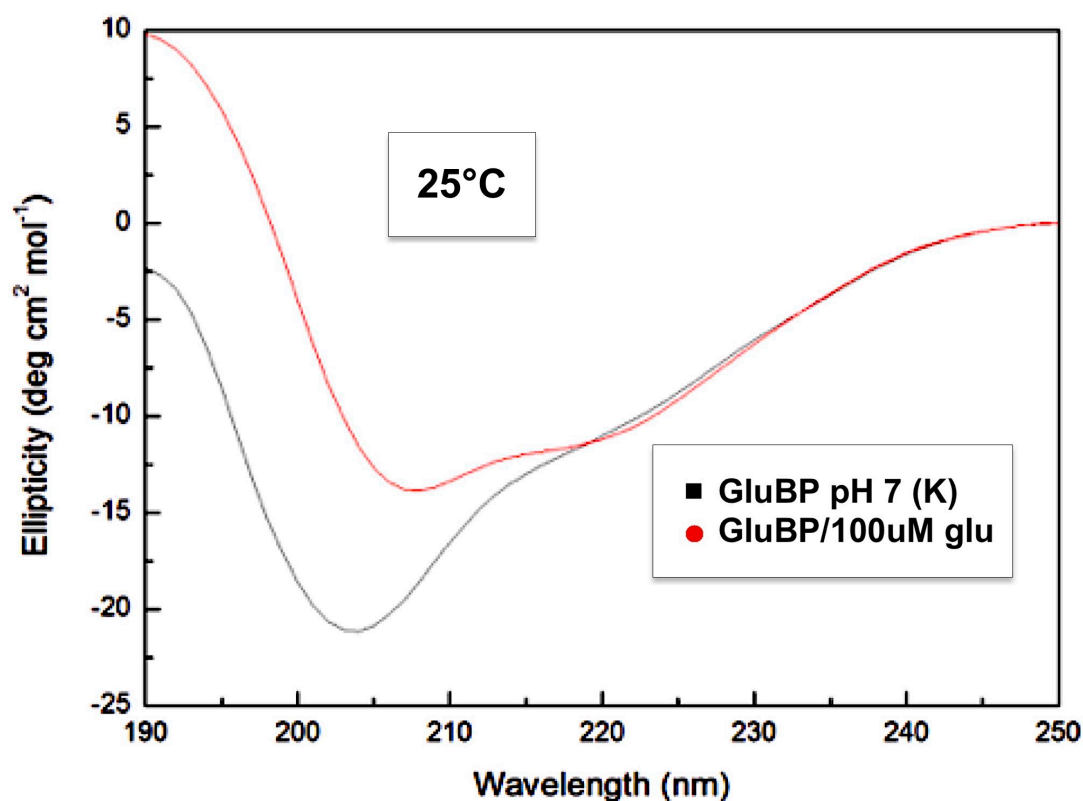
Thermal Scanning GluBP in (K$^+$) phosphate at pH 7

In order to understand the rate of formation of unordered peptide, values at 200 nm was plotted as a function of temperature as it shown in Figure 15B. In the absent of glutamate and sodium large amount of unordered proteins were shown by spectra early with faster decrease of ellipticity at 200 nm and increase at 222 nm (blue rows). Spectra have a plateau at 50-55 °C (200 nm and 222 nm) and slightly increase up to 80 °C. In the presence of glutamate less amount of unordered proteins were shown and an increase of α −helical content as shown by higher negative value of ellipticity at 222 nm and by spectra with slower decrease of ellipticity at 200 nm and increase at 222 nm (blue rows). Spectra have a plateau at 60-55 °C (at 200 nm and 222 nm). Very interesting to note after added mono sodium L-glutamate (MSG) at 100 µM diluted in the same buffer, protein structure changes and lower content of unordered structure appear at 24 °C as it was shown in Figure 15. In this experiment content of α −helical was reduced in the presence of 20 mM potassium phosphate and increase in presence of glutamate as shown by increase value of ellipticity at 222 nm. β −sheet content (green rows) as is shown in figures 16 A and B is stable in the absence and in the presence of glutamate at 24 °C as demonstrated by stable values (-17) of ellipticity at 216 nm characteristic of this secondary structure but decrease slowly in the presence glutamate during thermal scans. Spectra obtained by the protein in this buffer remark the same protein at higher temperature in sodium phosphate buffer (See Figure 18). The presence of mono sodium glutamate at 100 µM and consequently added sodium at the same concentration as shown in Figure below did not remark spectra of GluBP in 20 mM sodium phosphate buffer. This data suggests that the glutamate-binding affects the secondary structure of GluBP but they not explain all structural changes occurred during experiment in different phosphate buffer. In is very interesting to note that are present in both experiments an isosbestic point at 206 nm characteristic of two-state transition model might of α −helical content in random coil structures anyway β −sheet structures are more stable than α −helical structures in thermal scam experiments.

Figure 16: CD Spectra Thermal Scans
GluBP GluBP/glutamate complex (A and B respectively) in the presence of 20 mM potassium phosphate buffer; in grey circles were shown a magnifier images of spectra around 222 nm and 200 nm in the absence and in the presence of glutamate respectively; percent ellipticity at 200 and 222 nm were plotted in a function of temperature.

GluBP/glutamate and interferents complex in (Na$^+$) phosphate buffer

All proteins spectra show an intense negative band from 208 to 225 nm and a strong positive band about 190 nm. α/β Proteins generally have spectra dominated by the α-helical component and, therefore, often show bands at 222, 208, and 190–195 nm but in this cases, was observed a single broad minimum between 210 and 220 nm because of overlapping $\alpha -$helical and $\beta -$sheet contributions. Otherwise regular all $-\beta$ proteins usually have a single negative band (210–225 nm) and a stronger positive band (190–200 nm); instead in GluBP spectra the intensities of these bands reflect both α-helical and β-sheet contribution. Added glutamate at pH 8 changes slightly properties spectra and the shape in all wavelengths observed and α-helical content (20.8%) slightly increases (28.3%) instead and β-sheet content (43.0%) slightly decrease (34.6%). Instead at pH 7 added glutamate did not change dramatically properties spectra but the shape in all wavelengths observed and α-helical content (40.3%) slightly increase (54.5%) instead and $\beta -$sheet content are stable (about 40%). Structures of GluBP at pH 8 slightly increase of $\alpha -$helical and turn content and slightly decrease of β -sheet and also decrease of unordered content (random). $\alpha -$helical structures at pH 7 are higher (40.3%) than at pH 8 (20.8%), and slightly increase in the presence of L-glutamate at pH 7 (54.5%) and also at pH 8 (34.6%). It is interesting to note that at pH 7 in presence of glutamate decrease random structures and structures turn were absent. Instead $\beta -$sheet content at pH 8 was stable about 28% GluBP and GluBP/glutamate complex. Interesting amount of α-helical GluBP/complex at pH 7 is higher than at pH 8, but in the presence of glutamate increase higher (increase about 15%) than GluBP/glutamate complex at pH 8 (increase about 8%). Also GluBP/glutamate complex increase $\alpha -$helical and turn content while β-sheet and random content decrease as a consequence of binding of ligand (glutamate) and formation of close form typically of this protein family.

In order to study the stability of the protein, we investigated the effect of the temperature on the secondary structure of GluBP. Far-UV CD measurements in the range of temperature from 25 to 80 °C were performed in the absence and in the presence of 100 μM glutamate in buffer sodium phosphate at pH 7 and pH 8. Also in this case, as in GluB lipoprotein, reduced amount of salt dialyzed at pH 7 for CD experiments, part of protein precipitated and lost during centrifugation. Instead protein stock in the presence of 300 mM NaCl in buffer sodium phosphate buffer at pH 8 and pH 7 is stable for several months at 4 °C. In order to understand the batch of formation of α −helical content values at 222 nm were plotted in a function of temperature and Tm has been graphically calculated (See Figure 18B). It has been very interesting to note after adding MSG at 100 μM diluted in the same buffer, how protein structure slightly change and lower content of unordered structure disappeared appear at 25 °C as it was shown in Figure below. Also, in this case as in buffer potassium phosphate in presence of glutamate Tm_{222} of GluBP complex was higher than GluBP alone. Spectra obtained by the protein/complex at higher temperature remark GluBP alone at low temperature in the same buffer. The content of α-helical was found to significantly decrease with increasing temperature; the decrease being slightly lower for GluBP/glutamate complex than for GluBP alone and it means that protein complex was more thermal stable than protein alone.

**Table 2: Percent secondary structures of GluBP and GluBP/glutamate complex at pH 7 and pH 8 (25, 50 and 80 °C)**

pH 7				
*pH 7 + glu	α-Helix	β-Sheet	Turn	Random
25°C	40.3%	41.6%	2.8%	15.3%
*25 °C	*54.5%	*39.9%	*0.0%	*5.6%
50°C	4.8%	49.3%	3.8%	42.0%
*50 °C	*38.5%	*41.9%	*2.7%	*16.9%
80°C	0.0%	47.4%	4.5%	48.0%
*80 °C	*0.0%	*43.7%	*5.4%	*50.9%

pH 8				
*pH 8 + glu	α-Helix	β-Sheet	Turn	Random
25°C	20.8%	43.0%	7.5%	28.6%
*25°C	*28.3%	*34.6%	*10.0%	*27.1%
50°C	0.0%	39.2%	10.8%	50.0%
*50°C	*19.1%	*36.0%	*8.9%	*36.1%
80°C	0.0%	45.1%	7.1%	47.8%
*80°C	*0.6%	*42.9%	*8.2%	*48.2%

Figure 17 Upper. GluBP and GluBP/glutamate complex CD spectra (25°C) in the presence of sodium (Na⁺) phosphate buffer at pH 7 and pH 8
Lower. Thermal scan CD spectra of GluBP and GluBP/glutamate complex in the presence of sodium (Na⁺) phosphate buffer at pH 8 and pH 7.
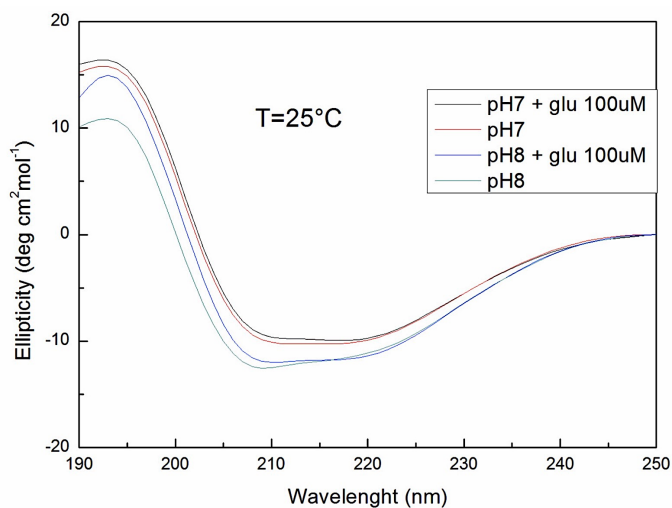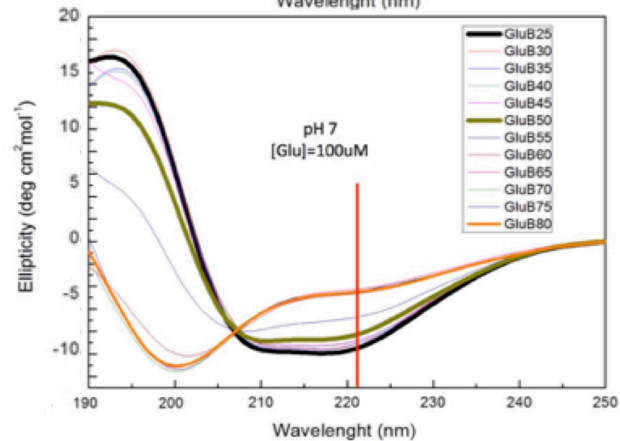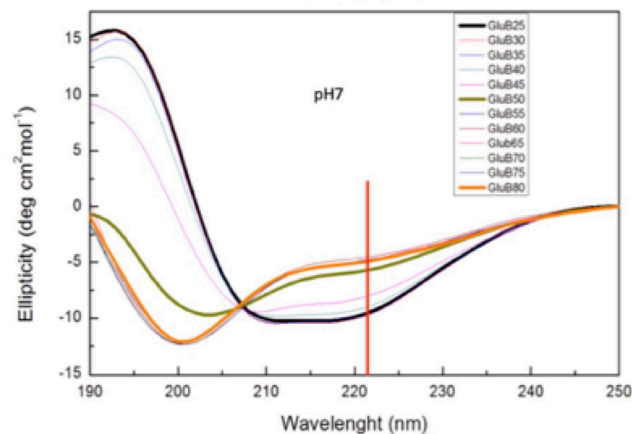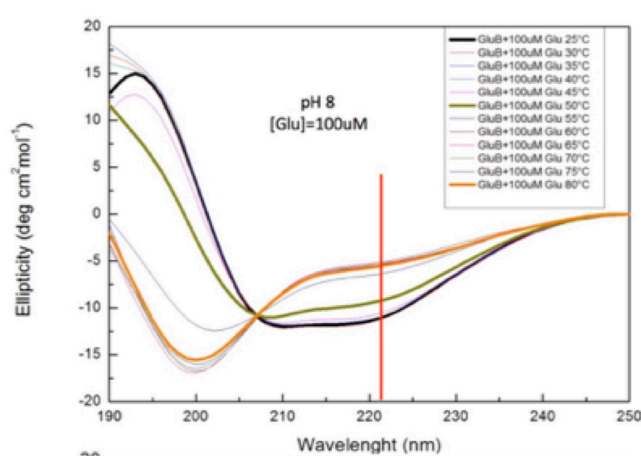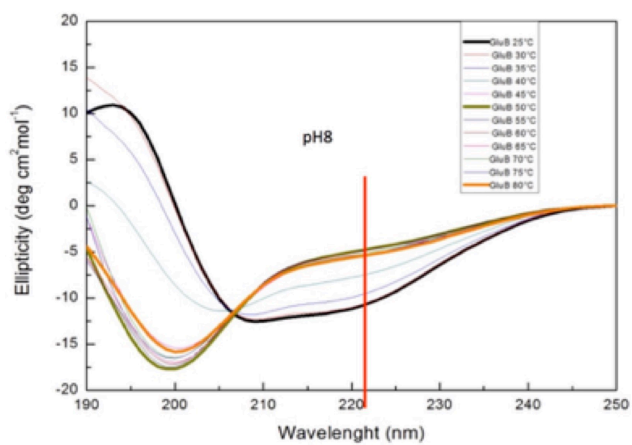

pH8	Helix	Beta	Turn	Random	Total
25°C	**20.8%**	**43.0%**	7.5%	28.6%	100%

pH7	Helix	Beta	Turn	Random	Total
25°C	**40.3%**	**41.6%**	2.8%	15.3%	100%

pH8+glu	Helix	Beta	Turn	Random	Total
25°C	**28.3%**	**34.6%**	10.0%	27.1%	100%

pH7+glu	Helix	Beta	Turn	Random	Total
25°C	**54.5%**	**39.9%**	0.0%	5.6%	100%

It is interesting to note that at 60 °C was obtained almost identical CD spectra from both the GluBP and the GluBP/glutamate complex, CD Spectra resulting look like at pH 7 and 8. The observation suggests that at 60 °C the protein is in a similar state independently of the presence of 100 μM glutamate and arrive to a plateau with a slightly increase values of ellipticy at 200 in unordered content. Also at lower temperature is observed a plateau interrupted ad 35 °C and 45 °C in GluBP/glutamate complex and GluBP respectively. Moderate changes in the Far-UV CD for GluBP temperature increase up to 35 °C indicate minor secondary structure alterations in the protein structure than in GluBP in buffer potassium phosphate (data not shown). Such changes are indicated by an initial decrease in the Far-UV CD negative signal at 222 nm and a slight decrease negative signal at 200 nm after a plateau for all spectra later 60 °C. β –sheet up to 80 °C is stable at pH 7 and pH 8 during thermal denaturation with a mean of 43%; β –sheet content at 50 °C slightly decrease at pH 8 an slightly increase at pH 7. Tm graphically calculated was about 55 °C, both at pH 7 that at pH 8. In the absence of glutamate was higher at pH 7 (about 45 °C) than at pH 8 (about 40 °C). The obtained data show that the addition of glutamate determines an increase of the thermal stability of GluBP. In the presence of L-glutamate stabilizes the structure of GluBP of about 10 °C at pH 7 and 5 °C at pH 8.
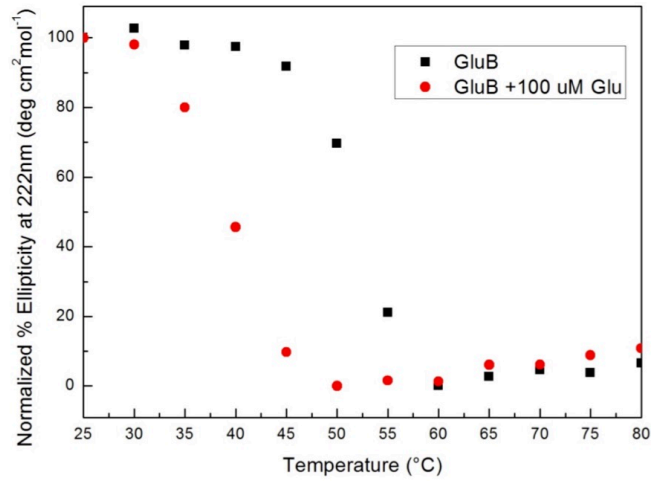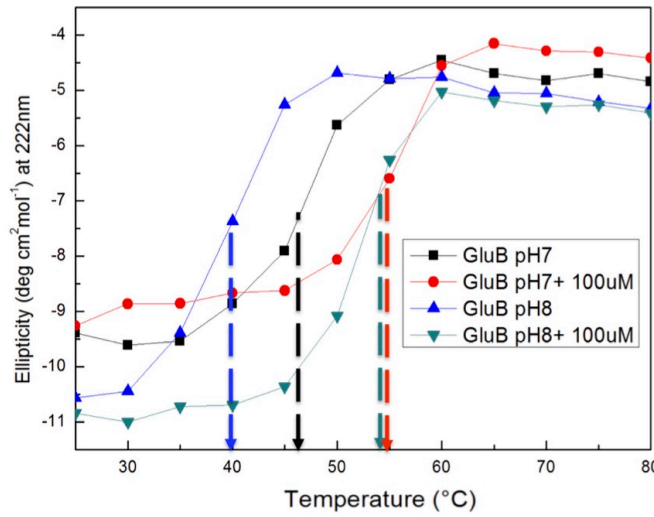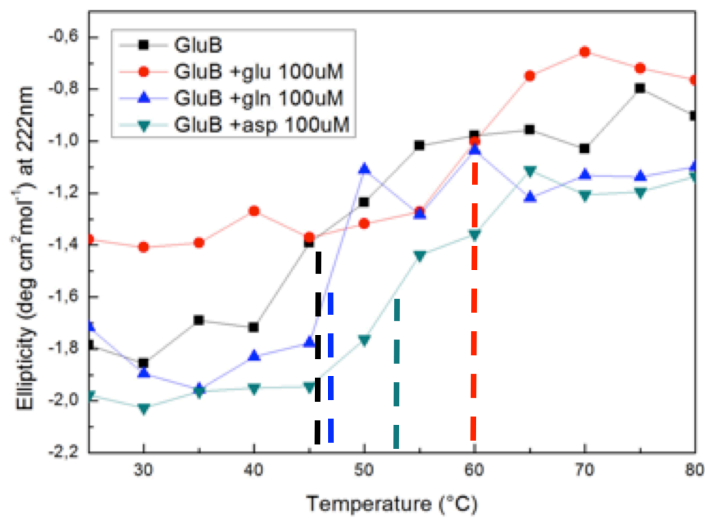
Figure 18: Temperature of melting at 222 nm
Normalized % Ellipticity at 222 nm at pH 8 (A); Temperature of melting GluBP and GluBP/ glutamate complex at pH 7 and pH 8 in the presence of sodium (Na$^+$) phosphate buffer (B); Temperature of melting of GluBP and GluBP/interferent at pH 8 in the presence of sodium (Na$^+$) phosphate buffer (C).

GluBP/glutamate vs GluBP /interferent complex in (Na$^+$) phosphate buffer at pH 8

In order to study the specificity of the GluBP for L-glutamate, we investigated the effect of the temperature on the secondary structure of GluBP in the presence also of other aminoacids. Far-UV CD measurements in the range of temperature from 25 to 80 °C were performed in the absence and in the presence of 100 μM of L-glutamate, L-glutamine and L-aspartate in buffer sodium phosphate at pH 8. Concentration of GluBP in these experiments was reduced to increase ratio analyte/protein to obtain more stringent binding conditions. The obtained data show that the addition of L-glutamate and L-aspartate determines an increase of the thermal stability of GluBP, no effect was observed in the presence of L-glutamine. L-glutamate stabilizes the structure of GluBP of about 10 °C in the presence of L-aspartate Tm increases of 5 °C instead (See Figure 18C). This result confirms higher substrate specificity for L-glutamate.

## Steady-State Fluorescence Spectroscopy Spectra

The primary sequence of GluBP contains two tryptophan residues at N-term (See Figure 9: W86 and W93). Because tryptophan emission is highly sensitive to its microenvironment, it can be used as an excellent intrinsic probe since these two amino acid residues are highly sensitive to their microenvironment they can be used as intrinsic probe for investigation of the conformational changes in protein structures (Herman *et al.* 2004).

GluB lipoprotein glutamate titration in buffer (K$^+$) phosphate at pH 7

In order to investigate tertiary structure of GluB lipoprotein, experiments of Steady-State fluorescence were performed. For the fluorescence measurements to determine the perturbation on tryptophan residues alone (without tyrosine contribution), the excitation wavelength was fixed at 295 nm. In order to perform experiments of binding of glutamate to GluB lipoprotein, we used increasing concentration of glutamate (0-33 μM) to determine the minimum and maximum concentration that has effect on the protein. In experiments performed at RT we observed a reduction of fluorescence intensity with 3 nM glutamates (data were corrected for dilution) after incubation of 30 minutes; while with 33 μM glutamate we have the same affect of 3 μM glutamate. This results by using equation 1 allow the calculation of apparent binding costant of 6±4 nM (see Figure 19). Only with overnight incubation experiment at 4 °C it is possible to observe a blue-shift in maximum emission, as it possible to observe in fluorescence spectra by ON incubation (See Figure 20) and and not obseved in 30 min incubation (See Figure 19) of binding with glutamate; as a consequence of a reduced solvent accessibility to the tryptophans. In Figure 20A are shown the fluorescence emission spectra of the GluB lipoprotein in the absence and in the presence of 100 μM glutamate at RT after overnight incubation at 4 °C. The results show that the fluorescence maximum emission of GluB lipoprotein in the absence of the glutamate is centered at 337 nm.

Comparing the fluorescence spectrum of GluB protein with fluorescence spectrum of N-acetyltryptophanamide (NATA), a tryptophan derivative whose maximum fluorescence wavelength excitation and emission were respectively at 295 nm wavelength 350 nm, it can be concluded that the tryptophan residues are in an environment not exposed to the solvent and un-relaxed. The GluBP/glutamate complex spectrum presents a peak centered at 331 nm in potassium phosphate and 337 nm in sodium phosphate buffer pH 8 as shown in thermal scan experiments. The fluorescence maximum emission (with excitation at 295 nm) is blue-shifted at pH 7. This indicates that the addition of 100 μM of ligand determines a conformational change in the protein.

Figure 19: Glutamate titration 30 min binding experiment at RT from 0 to 33000 nM (33 μM) glutamate (C) both in buffer potassium phosphate pH 7
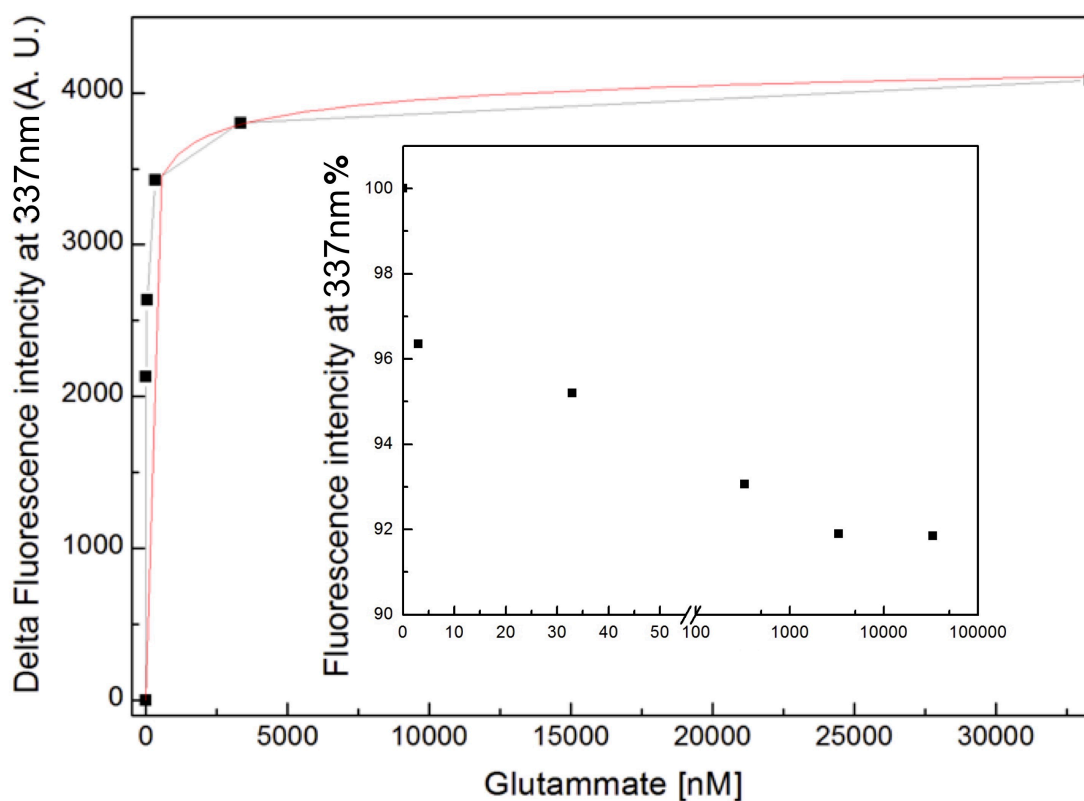
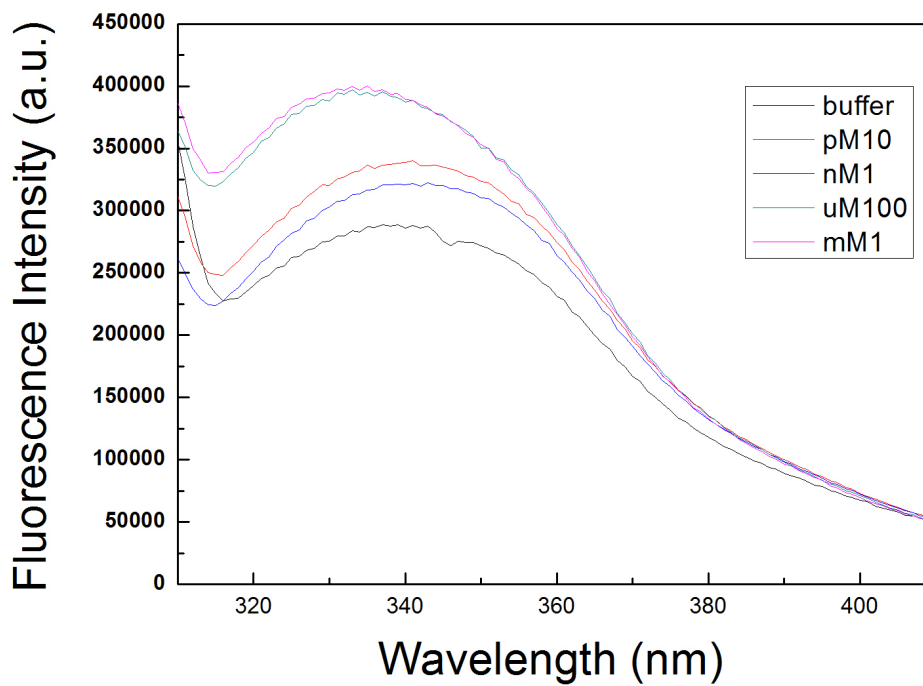**Figure 20: Normalized spectra at 0 and 100 μM glutamate (A) and glutamate titration ON binding experiment at 4 °C from 0 (buffer), 10 pM (pico), 1 nM, 100 μM and 1 mM of glutamate both in buffer potassium (K$^+$) phosphate pH 7**
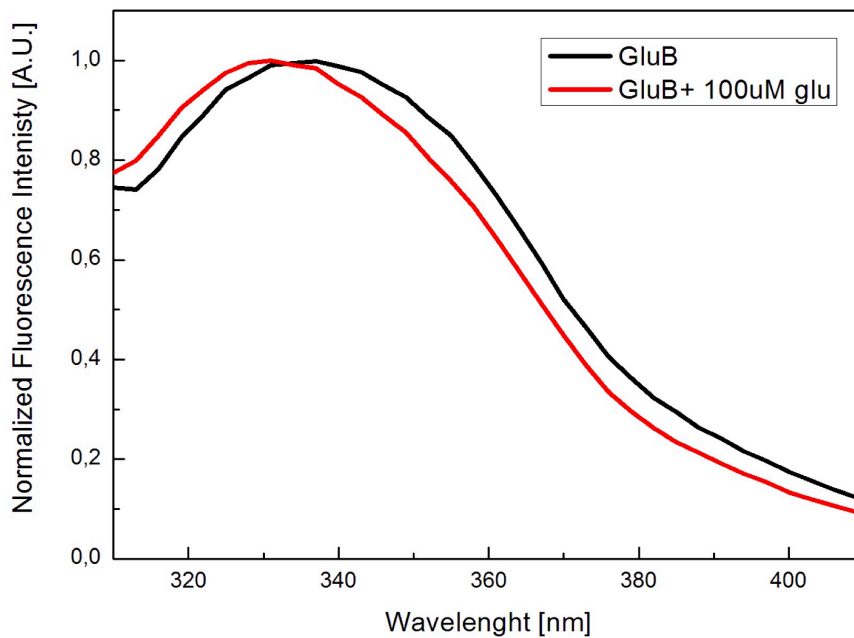

A

B

Thermal Scanning Fluorescence Spectra (W) of GluBP/lipoprotein the absence and the presence of L-glutamate dissolved in buffer (K$^+$) phosphate at pH 7

The effect of the temperature on the tertiary structure of GluBP was investigated by fluorescence measurements in the range of temperature 25-90 °C in the absence and in the presence of 100 μM L-glutamate in buffer potassium and sodium phosphate. Fluorescence emission maximum wavelength of GluBP tryptophan at the 337 nm (331 nm in binding overnight of 100 μM glutamate), as shown in Figure 21 moderately increases at temperature less than 45 °C. In contrast, the tryptophan fluorescence maximum wavelength quickly increases at temperature higher than 50 °C up to the GluBP emission wavelength at 350 nm (See Figure 21). GluBP maximum emission wavelength visibly rises with the initial temperature increase to 55 °C, which is the temperature that yields the fluorescence emission wavelength maximum. By increasing the temperature up to 90 °C, the maximum emission wavelength value for GluBP increased slightly. As shown by Figure 21A and Figure 21B, in the presence of 100 μM glutamate (A) the protein structure is stabilized. In fact the T$_m$ increases from about 40 °C to about 50 °C (Standard Deviation of three different experiments). In Figure 22A are shown the fluorescence emission maximum wavelength plotted as a function of temperature, in the absence and in the presence of 100 μM glutamate. No different in maximum intensity fluorescence emission was observed during thermal scans in the presence and in the absence of glutamate (See Figure 22B).

Figure 21: Fluorescence thermal scans of GluBP (A) and GluBP/glutamate complex (B) in buffer k$^+$ phosphate at pH 7
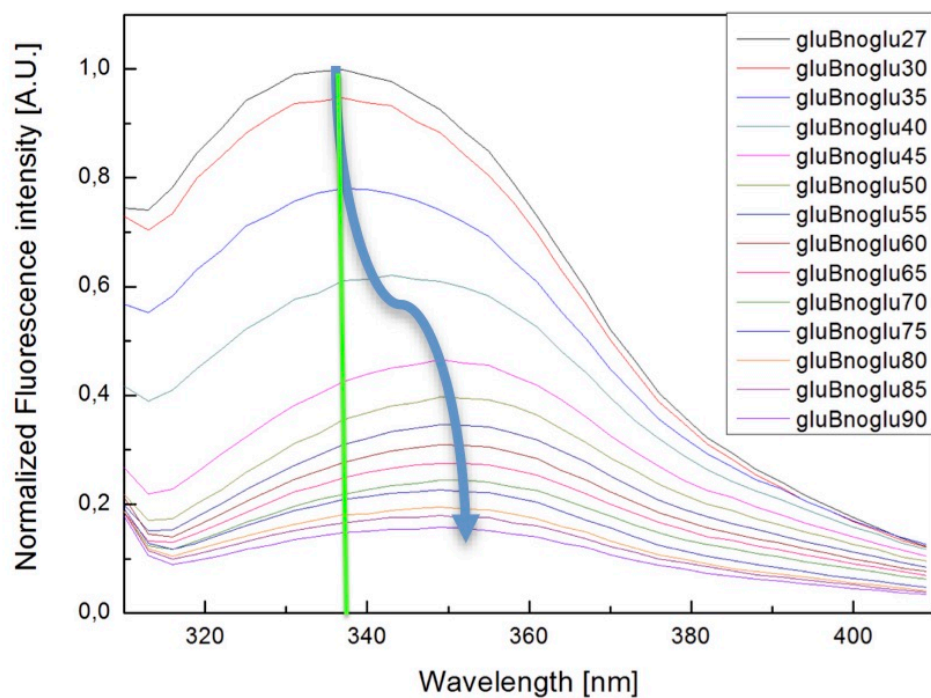

A
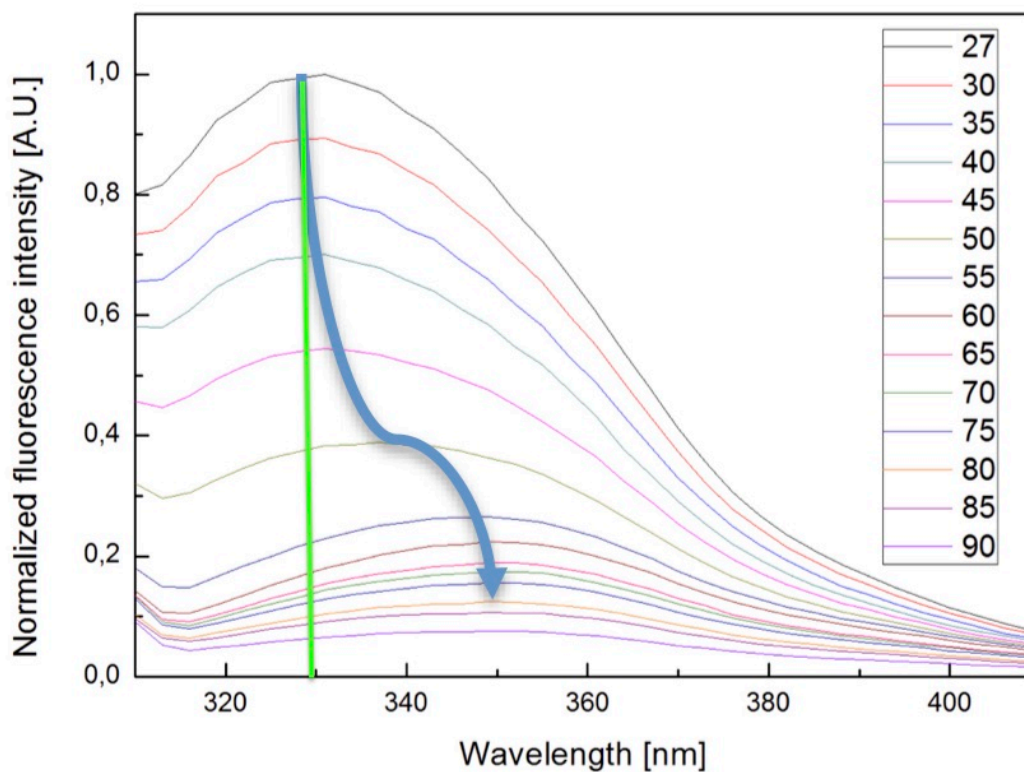
B

Fluorescence Transition Two-state Model

Emission wavelength at 337 nm (331 nm GluBP/glutamate complex) as shown in Figure 21 is stable at temperature less than 35 °C (45 °C in GluBP/glutamate complex). In contrast, wavelength quickly increases at temperature higher than 35 °C (45 °C in GluBP/glutamate complex) up to the GluBP maximum emission wavelength of 350 nm at 45 °C (55 °C GluBP/glutamate complex). GluBP maximum emission wavelength visibly rises with the initial temperature increase to 45 °C (55 °C GluBP/glutamate complex), which is the temperature that yields the emission maximum wavelength. By increasing the temperature up to 90 °C, the maximum emission wavelength value for GluBP were stable. In Figure 22A are shown the fluorescence emission maximum wavelength plotted in a function of temperature, in the absence and in the presence of 100 μM glutamate. As shown in Figure 22A, in the presence of 100 μM glutamate the protein structure is stabilized. In fact the T_m increases from about 40 °C to about 50 °C. Instead as shown in Figure 22B no difference in maxima intensity fluorescence emissions was observed during thermal scans in the presence and in the absence of glutamate at each temperature.

These data suggest that high temperature-induced unfolding of recombinant GluBP is a two-state process, and structural perturbations at temperature below 35 °C (45 °C GluBP/glutamate complex) indicate that two intermediate states are formed at 35 (45 °C GluBP/glutamate complex) and 45 °C (55 °C GluBP/glutamate complex) (See Figure 21). The tryptophan fluorescence maximum emission for GluBP increased in a two-step mode in buffer potassium (K^+) phosphate (in the absence and in the presence of glutamate) in the temperature range between 25- 90 °C with two-plateau at 35 and 45 °C (45 and 55 °C in the presence of 100 μM L-glutamate) and a maximum at approximately 45 °C (55 °C in the presence of 100 μM L-glutamate) for the GluBP tryptophan fluorescence maximum emission wavelength curve (Figure 22) on spectra observed in Figure 21.

Figure 22: GluBP/glutamate complex maximum emission wavelength and fluorescence intensity in a function of temperature

A

B
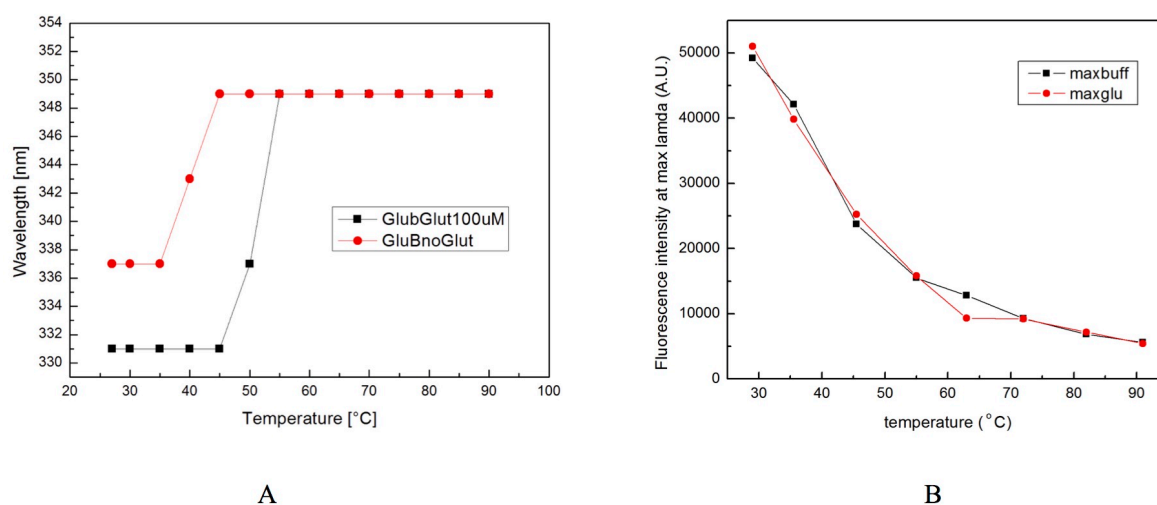
The pH effect from pH 6 up to pH 8 on GluBP intrinsic Fluorescence (W) in (Na$^+$) phosphate buffer

The perturbations of the proteins at different pH causes the destabilizing of intra-molecular repulsive interactions between same charges (Murkherjee *et al*. 2008), pH can influence the conformation and the stability of the protein because it alters the net charge on the protein. In order to investigate the emission spectra of two Triptophans (Trp, W) in different microenvironment influenced by different pH (from pH 6 up to pH 8 with increase of 0.5 pH) in the same buffer solution, GluBP samples were incubated overnight in the same buffer at different pH and Fluorescence steady state measurements were performed at RT. The results are shown in Figure 23. From these spectra, it can be deduced that the pH has an effect on the tertiary structure of the GluBP, as it deviates from the spectrum of NATA, which is centered at 350 nm and that is emission of Trp on surface of protein. We observed at value of pH lower than 7 pH a blue shift (up to 331) of maximum wavelength emission and increasing fluorescent intensity as shown in overnight binding experiments in the presence of glutamate; instead value of pH higher pH 7 showed a red-shift up to 337 nm as shown in GluBP in the absence of glutamate; as a consequence of changing microenvironment condition around the two Trp. It was very interesting to note that fluorescent spectrum of GluBP at pH 6 was very similar to GluBP in the presence of 100 μM of L-glutamate at pH 7 in potassium (K$^+$) phosphate.

Figure 23: pH effect on Maximum emission wavelength of GluBP in the presence of sodium phosphate buffer
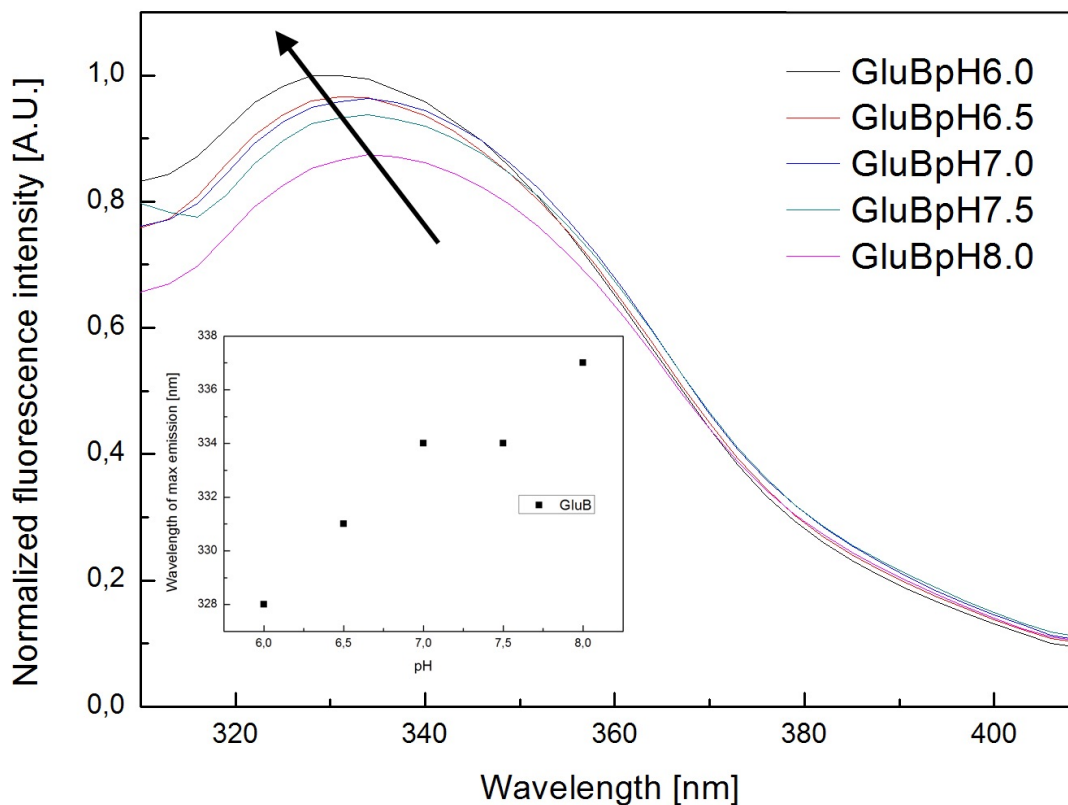
Fluorescence Quenching

Fluorescence quenching is the phenomenon whereby the fluorescence intensity of a sample decreases. In order to that quenching occurs, it is necessary that fluorophore and quencher need to be in contact. For this reason, quenching measurements reveal the accessibility of the fluorophores into quenchers: if the fluorophore is localized in the interior of the protein, quenching does not occur. A wide variety of molecules acts as quencher. One of these, of the indole, tryptophan and its derivate, is acrylamide. The use of the quenchers in protein of fluorescence allows to determinate where the tryptophans are localized in a protein. Quenching results were shown as plots of F_0/F versus [Q], because F_0/F should increase linearly with quencher concentration. If there are two population of fluorophore and one class is not accessible to quencher, the Stern-Volmer plots may not be linear. This is typical of the protein where the quencher can bind only to the tryptophan on the surface. In this way, quenching fluorescence can give structural information about the degree of the exposure of the tryptophan (Lakowicz 2006). In order to determine the tryptophan accessibility

to quencher in different conditions, acrylamide experiments on GluBP were performed at 25 °C and 50 °C, in the absence and in the presence of glutamate.

Stern-Volmer Quenching

We used acrylamide-induced fluorescence quenching to evaluate the solvent accessibility of the tryptophan residues of the protein. The intrinsic protein fluorescence was excited at 295, and the emission was monitored at 337 nm (330nm in the presence of 100 μM L-glutamate). The data generated were corrected based on the solvent signal. Previous studies have demonstrated the need to include the ratio W0/W if the quencher absorbs at the excitation wavelength (D'Auria & Lakowicz 2001). Acrylamide quenching of the tryptophan (Trp) fluorescence was observed at fluorescence maximum and analysed by the Stern-Volmer equation:

Equation 2

$$\frac{F_0}{F} = 1 + K_{sv}[Q]$$

Where K_{sv} is the Stern-Volmer quenching constant and $[Q]$ is the quencher concentration and the subscript **0** indicates the absence of a quencher (Mukherjee *et al*. 2008).

To evaluate Trp residue accessibility to quencher, we performed acrylamide quenching experiments at RT in the absence and in the presence of L-glutamate (100 μM). Values of K_{sv} for tryptophan fluorescence quenching by acrylamide are low and similar quenching rate with GluBP in the absence and in the presence of 100 μM L-glutamate, indicating that GluBP tryptophan residues in such states are not solvent accessible. As shown, the Stern-Volmer constants, as consequence of glutamate addition, K_{sv} slightly differ for the liganded and the unliganded form of GluBP; K_{sv} 4.3 and 6.2 M^{-1}. The results are presented in Figure 24. Black and red circles denote GluBP and the GlnBP/glutamate complex, respectively. The increase of acrylamide quenching of Trp emission suggests that the Trp residues become more accessible to solvent following ligand-bound at RT in the presence of 100 μM L-glutamate at pH 8.

Figure 24: Glutamate-binding induced quenching at pH 8 of GluBP and GluBP/glutamate complex
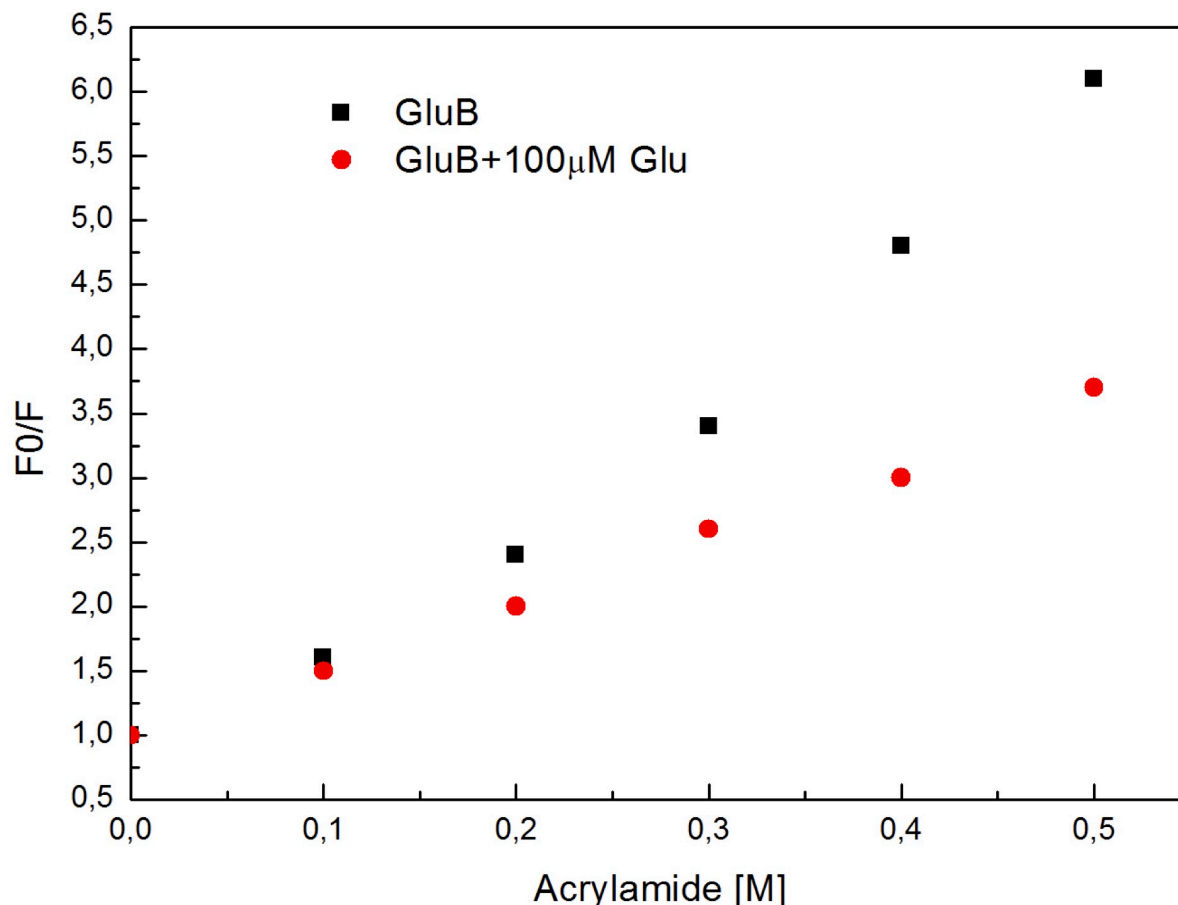
ANS Fluorescence measurements

We investigated also the effect of pH and binding of L-glutamate on the tertiary structure of GluBP by monitoring exposition of hydrophobic regions of GluBP. For this purpose, the binding of the 8-anilino-1-naphthalenesulfonic acid (ANS) to the GluBP, at a different pH and in the presence of L-glutamate, were determined by the steady state fluorescence experiments. The ANS is a fluorescent probe utilized for the characterization of protein binding sites. It is able to bind to hidden hydrophobic sites of proteins. The hydrophobicity of the binding site and the restricted mobility of ANS determine a blue shift of fluorescence emission maxima and an increase of fluorescence (Stryer *et al.* 1965*)*. This enhancement of fluorescence is due to the interaction between sulfonate group of the ANS and the charged group of lysine and arginine. Ion pairing formed reduces the intermolecular charge transfer rate constant that leads to enhancement of fluorescence (Gasymov *et*

al. 2007) The ANS experiments were performed on GluBP samples at pH 2.0, pH 7.0 and pH 11.0. GluBP was diluted with buffer at different pH, so that the absorbance at 295 nm was 0.1 OD. In order to moles of the ANS were more than 10-fold greater than the mole of the protein, an excess of ANS was added. The excitation wavelength of 370 nm, which is the wavelength of absorption of the ANS, was used for this experiment. The obtained results are shown in Figure 25 GluBP at pH 2.0 is completely denatured because the hydrophobic residues, that bind the ANS, are completely exposed on the surface and the ANS emission is maximum; at pH 7.0 and pH 11.0 there are no peak corresponding to the emission wavelength of the ANS and so GluBP, at these pH values, do not expose hydrophobic regions also at pH 11. It was also performed binding experiment at pH 8 in the absence and in the presence of L-glutamate and as it was possible to observe in Figure 25B in the presence of L-glutamate ANS fluorescence increases and it means that hydrophobic regions of GluBP were exposed during binding state and they can be bound by the ANS.

Figure 25: ANS binding fluorescence measurements of GluBP at pH 8 in the absence and in the absence of glutamate (A); and ANS binding fluorescence measurements at extremes pH

A

B
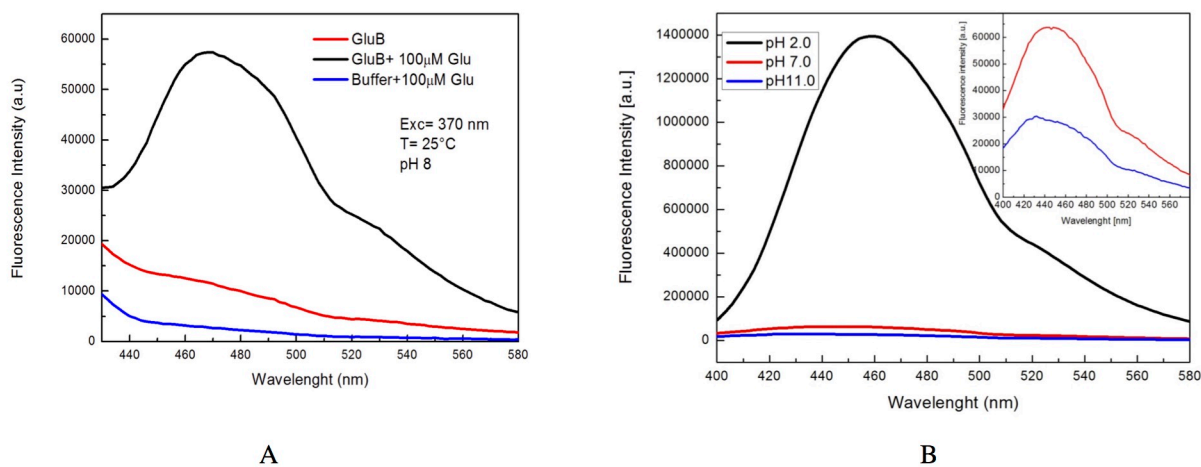
SDS/Native PAGE and Size-Exclusion Chromatography

In order to investigate quaternary structure of GluBP two different experiments were performed at pH 8.3: Native PAGE and Size-exclusion chromatography. The former gave as an overview of protein pattern of GluBP incubated with different buffer solution before PAGE. In this experiment, the migration was obtained by net negative charge and shape of protein complex. In native PAGE, gel mobility of GluBP (major band, IP= 4.2) was faster than Ovalbumin (PI= 4.5). It means that shape of GluB Protein (major band) was smaller than Ovalbumin (45 KDa). This result gave as evidence that a large amount of GluBP was a monomer (about 32 KDa with His-Tag) in this

experimentally conditions. There were also other bands at higher molecular weight as shown in Figure 26B. The results of PAGE showed different peaks blue rows in different concentration of NaCl in samples. It is possible that these bands were dimers of GluBP and that this protein has a quaternary structure. This hypothesis was tested by size-exclusion chromatography by comparing chromatograms of GluBP gel mobility in different concentration of salt (NaCl) by gel filtration (50 mM Tris pH 8.3). The chromatograms overplayed of the three runs in different conditions were normalized as shown in Figure 26A. In high (500 mM-blue line) and low concentration of salts (150 mM-black line) there were two peaks: minor (about 10%) peak (higher shape) was eluted before (after 30 ml of buffer) and major peak (lower shape) eluted after 35 ml of respectively buffer. In presence of low salt concentration the same ratio major/minor peak was conserved but major peak was slightly shifted and elute before (about 33 ml) since GluBP shape in this condition was higher than in high salt concentration. Moreover it is possible observe a single peak at the highest shape in the absence of salts. It means that, GluBP (in the absence of NaCl), gel mobility results in a single peak with higher shape than in presence of NaCl. These results suggest that GluBP has a quaternary structure influenced by ionic strength of running buffer. Also in GluBP SDS-PAGE described before gel mobility of GluBP was shown in Figure 27; as it possible to observe also in this experiment protein samples of GluBP were influenced by ionic strength and pH before native PAGE run. In this experiment pH of buffer could influence net charge of protein also at higher concentration of NaCl (300 mM) increase a gel motility of GluBP as happen in the presence of buffer at pH 7 and in the absence of salts. These results suggest that the pH and the ionic strength influence not only secondary and tertiary structure but also quaternary structure of GluBP as it was possible observe in size-exclusion chromatography (50 mM Tris, with 0, 150 and 500 mM NaCl at pH 8.3) and Native PAGE (25 mM Tris, 192 mM glycine at pH 8.3) of GluBP.

Figure 26: Size-Exclusion Chromatograms of GluBP in the presence of increasing concentration of NaCl (A) and native PAGE 15% (B) both in Tris at pH 8.3

A

B
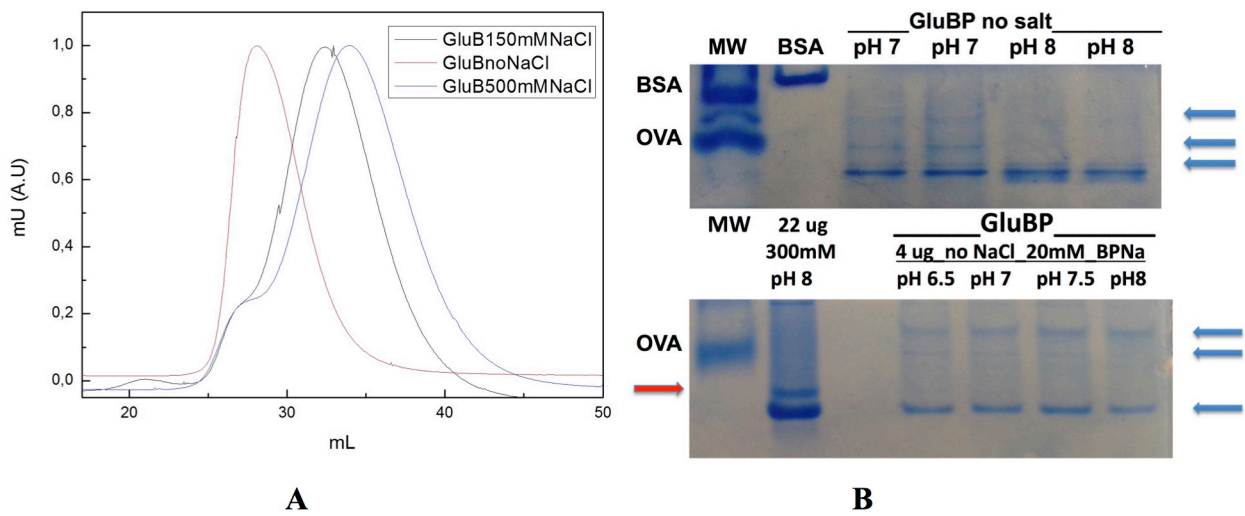
Figure 27: SDS-PAGE of GluBP in the presence and in the absence of high salt content at different pH
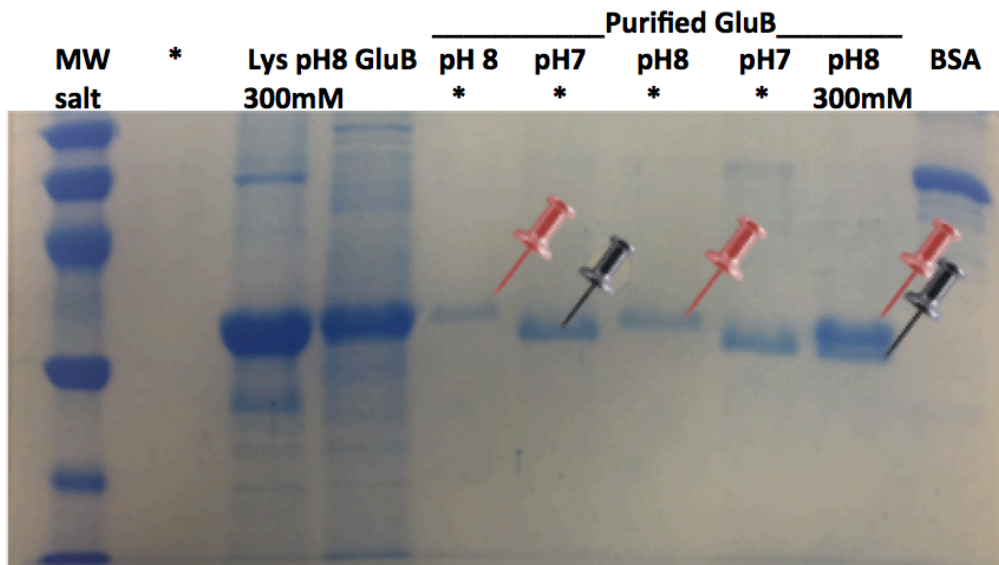
Conclusions

A Substrate-binding protein able to bind glutamate was isolated, cloned and expressed in a bacterial host. The structural characterization of GluBP was done using advanced spectroscopic techniques (CD and Steady-State Fluorescence measurements) in order to evaluate its behavior in the absence and in the presence of ligand and different cations at different pH. GluBP shows higher stability in presence of sodium than in potassium phosphate buffer with higher content of alpha-helical structures. Fluorescence binding experiment allows obtaining apparent binding constant of 6±4 nM. The presence of isosbestic point at 206 nm in thermal scan CD spectra suggests a two-state model of thermal denaturation, which involved alpha-helical and random coil structures. Also in fluorescence spectra thermal scans the presences of two-plateau and fast increase of fluorescence emission wavelength maximum indicate the fluorescence Transition Two-State Model. Temperature of melting (Tm) increase about 10 °C in the presence of L-glutamate both in CD that in Steady-State Fluorescence thermal scans. The obtained results of thermal stability from this study have revealed that GluBP is a potential candidate for development of biosensor for detection of glutamate. The glutamate-induced stability of the secondary and tertiary structure on GluBP and biochemistry characterization can be considered a starting point for the construction of biosensor. The development of a biosensor capable of a rapid detection of glutamate would be an important innovation. It is essential control glutamate levels in the human fluids and foods because of brain excitotoxicity. All these obatined results together with future resolution of tridimensional structure of GluBP will be useful for development of a FRET-fluorescent biosensor for L-glutamate in foods and human fluids.

References

Alloing, G., de Philip, P., and Claverys J., P. (1994) Three highly homologous membrane-bound lipoproteins participate in oligopeptide transport by the Ami system of the gram-positive *Streptococcus pneumoniae*. J Mol Biol. 241:44–58.

Ausili, A., Staiano, M., Dattelbaum, J., Varriale, A., Capo, A., D'Auria, S. (2013) Periplasmic Binding Proteins in Thermophiles: Characterization and Potential Application of an Arginine-Binding Protein from *Thermotoga maritima*: A Brief Thermo-Story. Life (Basel). Feb 5;3(1):149-60.

Bergles, D. E., Roberts, J. D., Somogyi, P., and Jahr, C. E. (2000) Glutamatergic synapses on oligodendrocyte precursor cells in the hippocampus. Nature. 11;405(6783):187-91.

Berkowitz, S. A., Engen, J. R., Mazzeo, J. R., and Jones, G. B. (2012) Analytical tools for characterizing biopharmaceuticals and the implications for biosimilars. Nat Rev Drug Discov. 29;11(7):527-40.

Berman, H. M., Westbrook, J., Feng, Z., Gilliland, G., Bhat, T. N., Weissig, H., Shindyalov, I. N., and Bourne, P. E., (2000) The Protein Data Bank. Nucleic Acids Res.; 28:235-42.

Bermejo, C., Ewald, J. C., Lanquar, V., Jones, A. M., and Frommer, W. B. (2011) In vivo biochemistry: quantifying ion and metabolite levels in individual cells or cultures of yeast. Biochem J. 15;438(1):1-10.

Berntsson, R. P., Smits, S. H., Schmitt, L., Slotboom, D. J., and Poolman, B. (2010) A structural classification of substrate-binding proteins. FEBS Lett. 18; 584(12): 2606-17.

Boos, W., and Lucht, J. M. (1996). Periplasmic binding protein-dependent ABC transporters, p. 1175–1209. In F. C. Neidhardt, R. Curtiss III, J. L. Ingraham, E. C. C. Lin, K. B. Low, B. Magasanik, W. S. Reznikoff, M. Riley, M. Schaechter and H. E. Umbarger (ed.), Escherichia coli and Salmonella: cellular and molecular biology. American Society for Microbiology. Washington, D.C.

Bornhorst, J. A., and Falke, J. J. (2000) Purification of Proteins Using Polyhistidine Affinity Tags. Methods Enzymol.; 326: 245-54.

Burkovski, A., Weil, B., and Krämer, R. (1996) Characterization of a secondary uptake system for L-glutamate in *Corynebacterium glutamicum*. FEMS Microbiol Lett. 15; 136(2): 169-73.

Busby, T. F., Atha, D. H., and Ingham, K. C. (1981) Thermal denaturation of antithrombin III. J Biol Chem 256(23):12140–12147.

Busby, T. F., Atha, D. H., and Ingham, K. C. (1981) Thermal denaturation of antithrombin III. Stabilization by heparin and lyotropic anions. Journal of Biological Chemistry. 256:12140–12147.

Chang, Z., Choudhary, A., Lathigra, R., and Quiocho, F. A. (1994) The Immunodominant 38-kDa Lipoprotein Antigen of *Mycobacterium tuberculosis* Is a Phosphate-binding Protein. J. Biol. Chem. Vol. 269, No. 3, 21, pp. 1956-1958.

Chen, Y.H., Yang, J. T, and Chau, K. H. (1974) Determination of the helix and β form of proteins in aqueous solution by circular dichroism. Biochemistry. 13(16): 3350-3359.

Clarke, G., O'Mahony, S., Malone, G., and Dinan, T. G. (2007) An isocratic high performance liquid chromatography method for the determination of GABA and glutamate in discrete regions of the rodent brain. J Neurosci Methods. 15; 160(2): 223-30.

Collingridge, G. L., Lester, R. A. (1989) Excitatory amino acid receptors in the vertebrate central nervous system. Pharmacol Rev. Jun;41(2):143-210.

Conti, G., Santarelli, R., Grassi, C., Ottaviani, F., and Azzena, G. B. (1999) Auditory steady-state responses to click trains from the rat temporal cortex. Clin Neurophysiol. 110(1):62-70.

Coulet, P. R., and Bardeletti, G. (1991) Biosensor-based instrumentation. Biochem Soc Trans. ;19(1):1-4.

D'Auria, S., and Lakowicz, J. R. (2001) Enzyme fluorescence as a sensing tool: new perspectives in biotechnology. Curr Opin Biotechnol.; 12(1): 99-104.

D'Auria, S., Di Cesare, N., Gryczynski, Z., Gryczynski, I., Rossi, M., and Lakowicz, J. R. (2000) A Thermophilic Apoglucose Dehydrogenase as Nonconsuming Glucose sensor. Biochem Biophys Res Commun.11; 274(3): 727-31.

Danbolt, N., C. (2001) Glutamate uptake. Prog Neurobiol. Sep;65(1):1-105.

Dattelbaum J.D., and Lakowicz J.R. (2001) Optical determination of glutamine using a genetically engineered protein. Anal. Biochem. 291:89–95.

Dattelbaum, J. D., and Lakowicz, J. R. (2001) Optical determination of glutamine using a genetically engineered protein. Anal Biochem. 1; 291(1): 89-95.

Davidson, A. L., Dassa, E., Orelle, C., and Chen J. (2008); Structure, Function, and Evolution of Bacterial ATP-Binding Cassette Systems Microbiol Mol Biol Rev. 72(2): 317–364.

Ding, F., Liu, W., Li, N., Zhang, L., and Sun, Y. (2010) Complex of nicosulfuron with human serum albumin: a biophysical study. J Mol Struct 975(1):256–264.

Dwyer, M. A., and Hellinga, H. W. (2004) Periplasmic binding proteins: a versatile superfamily for protein engineering. Curr Opin Struct Biol.; 14(4): 495-504.

Einspahr, H., Weiss, M. S., and Hunterc, W. N. (2013) Crystals on the cover 2014. Acta Crystallogr F Struct Biol Commun. 1; 70(Pt 1): 1.

Fonnum, F. (1984) Glutamate: a neurotransmitter in mammalian brain. J Neurochem.;42(1):1-11. Review.

Gasymov, O. K., and Glasgow, B. J. (2007) ANS Fluorescence: potential to augment the identification of the external binding sites of proteins. Biochim Biophys Acta.; 1774(3): 403-11.

Gilson, E., Alloing, G., Schmidt, T., Claverys, J. P., Dudler, R., and Hofnung, M. (1988) Evidence for high affinity binding-protein dependent transport systems in gram-positive bacteria and in Mycoplasma. EMBO J. 1;7(12):3971-4.

Grunewald, F.S. Periplasmic Binding Proteins in Biosensing Applications. BioanalRev. (2014); 1: 205-36.

Hamberger, A., and Nyström, B., (1984) Extra- and intracellular amino acids in the hippocampus during development of hepatic encephalopathy. Neurochem Res.;9(9):1181-92.

Hamdan, S. K., and Mohd Z. A. (2014) In vivo electrochemical biosensor for brain glutamate detection: a mini review. Malays J Med Sci. Dec; 21(Spec Issue): 12-26.

Headley, P. M., and Grillner, S. (1990) Excitatory amino acids and synaptic transmission: the evidence for a physiological function. Trends Pharmacol Sci. 11(5):205-11. Review.

Hellinga, H. W., and Marvin, G. J. S. (1998) Protein engineering and the development of generic biosensors. Trends Biotechnol. 16, 183–189.

Herman, P., Vecer, J., Scognamiglio, V., Staiano, M., Rossi, M., and D'Auria, S. (2004) A recombinant glutamine binding protein from *E.coli*: effect of ligand-binding on protein conformational dynamics. Biotechnol Prog.; 20(6): 1847-54.

Hernandez, L., Tucci, S., Guzman, N., and Paez, X. (1993) In vivo monitoring of glutamate in the brain by microdialysis and capillary electrophoresis with laser-induced fluorescence detection. J Chromatogr A 22; 652(2): 393-8.

Hirasawa, T., and Wachi, M. (2016). Glutamate Fermentation-2: Mechanism of L-Glutamate Overproduction in *Corynebacterium glutamicum*. Article 56 Advances in Biochemical Engineering/ Biotechnology 59 60 Adv Biochem Eng Biotechnol 3.

Hires, S. A., Zhu, Y., and Tsien, R. Y. (2008) Optical measurement of synaptic glutamate spillover and reuptake by linker optimized glutamate-sensitive fluorescent reporters. Proc Natl Acad Sci U S A. 18; 105(11): 4411-6.

Hollenstein K., Frei D. C. and Locher K. P. (2007) Structure of an ABC transporter in complex with its binding protein. Nature 446, 213-216.

Hösli, E., Hösli, L. (1993) Receptors for neurotransmitters on astrocytes in the mammalian central nervous system. Prog Neurobiol.; 40(4):477-506.

Hosseini M, Khabbaz H, Dezfoli AS, Ganjali MR, and Dadmehr M. (2014) Selective recognition of Glutamate based on fluorescence enhancement of graphene quantum dot. Spectrochim Acta A Mol Biomol Spectrosc. 1; 136PC: 1962-1966.

Jenkinson, H. F., Baker, R. A., and Tannock, G. W. (1996) A binding-lipoprotein-dependent oligopeptide transport system in *Streptococcus gordonii* essential for uptake of hexa- and heptapeptides. J Bacteriol.; 178(1):68-77.

Joshi, V., Shivach, T., Yadav, N., and Rathore, A.S. (2014) Circular dichroism spectroscopy as a tool for monitoring aggregation in monoclonal antibody therapeutics. Anal Chem. 2;86(23):11606-13.

Kaivosoja, E., Tujunen N., Jokinen, V., Protopopova, V., Heinilehto, S., Koskinen, J., and Laurila, T. (2015) Glutamate detection by amino functionalized tetrahedral amorphous carbon surfaces. Talanta. 15; 141: 175-81.

Kaupmann, K., Huggel, K., Heid J, Flor PJ, Bischoff S, Mickel SJ, McMaster G, Angst C, Bittiger H, Froestl W, Bettler B. Kaupmann, K. et al. (1997) Expression cloning of GABAB receptors uncovers similarity to metabotropic glutamate receptors. Nature QVTD 239±246 Nature. 20; 386(6622):239-46.

Kelly, A., and Stanley, C. A. (2001) Disorders of glutamate metabolism. Ment Retard Dev Disabil Res Rev.; 7(4):287-95.

Kelly, S. M., Jess, T. J., and Price, N. C. (2005) How to study proteins by circular dichroism. Biochim Biophys Acta. 10; 1751(2): 119-39.

Klenk, H. P., Clayton, R. A., Tomb, J. F., White, O., Nelson, K. E., Ketchum, K. A., Dodson, R. J., Gwinn, M., Hickey, E. K., Peterson, J. D., Richardson, D. L., Kerlavage, A. R., Graham, D. E., Kyrpides, N. C., Fleischmann, R. D., Quackenbush, J., Lee, N.H., Sutton, G. G., Gill, S., Kirkness, E. F., Dougherty, B. A., McKenney, K., Adams, M. D., Loftus, B., Peterson, S., Reich, C. I., McNeil, L. K., Badger J. H., Glodek, A., J. H., Zhou, L., Overbeek, R., Gocayne, J. D., Weidman, J. F., McDonald, L., Utterback, T., Cotton, M. D., Spriggs, T., Artiach, P., Kaine, B. P., Sykes, S. M., Sadow, P. W., D'Andrea, K. P., Bowman, C., Fujii, C., Garland, S. A., Mason, T. M., Olsen, G. J., Fraser, C. M., Smith, H. O., Woese C. R., and Venter J. C. (1997) The complete genome sequence of the hyperthermophilic, sulphate-reducing archaeon *Archaeoglobus fulgidus*. Nature 390, 364-370.

Kobayashi, K. F., Tateno Y., and Nishikawa K. (1999) Domain dislocation: a change of core structure in periplasmic binding proteins in their evolutionary history. Volume 286, Issue 1, 12 Pages 279–290.

Kronemeyer, W., Peekhaus, N., Krämer, R., Sahm, H., and Eggeling, L. (1995) Structure of the glu ABCD Cluster Encoding the Glutamate Uptake System of *Corynebacterium glutamicum*. J Bacteriol.; 177(5): 1152-8.

Laemmli, U. K., (1970) Cleavage of Structural Proteins during the Assembly of the Head of Bacteriophage T4. Nature; 227: 680-685.

Lakowicz, J. R. (2006). Principles of fluorescence spectroscopy. Third edition.. Springer Science+ Business Media, LLC.

Lehmann, A., and Hamberger, A. (1983) Dihydrokainic acid affects extracellular taurine and phosphoethanolamine levels in the hippocampus. Neurosci Lett. 15;38(1):67-72.

Lehmann, A., Isacsson, H., and Hamberger, A. (1983) Effects of in vivo administration of kainic acid on the extracellular amino acid pool in the rabbit hippocampus. J Neurochem. 40(5):1314-20.

Liu, Q., Li, D., Hu, Y., and Wang, d. C. (2013) Expression, crystallization and preliminary crystallographic study of GluB from *Corynebacterium glutamicum*. Acta Crystallogr Sect F Struct Biol Cryst Commun.; 69(Pt 6): 657-9.

Meldrum, B. S. (2000) Glutamate as a neurotransmitter in the brain: review of physiology and pathology. J Nutr.; 130 (4S Suppl): 1007S-15S.

Michel, A., Koch K. A, Krumbach, K., Brocker, M., and Bott, M. (2015) Anaerobic Growth of *Corynebacterium glutamicum* via Mixed-Acid Fermentation. Appl Environ Microbiol.;81(21):7496-508.

Montesinos, M. L., Herrero, A., and Flores E. (1997) Amino acid transport in taxonomically diverse cyanobacteria and identification of two genes encoding elements of a neutral amino acid permease putatively involved in recapture of leaked hydrophobic amino acids. J Bacteriol. ;179(3):853-62.

Moriyama, Y., Hayashi, M., Yamada, H., Yatsushiro, S., Ishio, S., and Yamamoto, A. (2000) Synaptic-like microvesicles, synaptic vesicle counterparts in endocrine cells, are involved in a novel regulatory mechanism for the synthesis and secretion of hormones. J Exp Biol. 203(Pt 1):117-25. Review.

Mukherjee, M., Ghosh, R., Chattopadhyay, K., and Ghosh, S. (2015) pH-induced structural change of a multi-tryptophan protein MPT63 with immunoglobulin-like fold: identification of perturbed tryptophan reside/residues. J Biomol Struct Dyn ;33(10):2145-60.

Mukherjee, V., Dutta A., and Sen, D. (2008) Defect generation in a spin-1/2 transverse X/Y chain under repeated quenching of the transverse field. Phys. Rev. B 77, 214427.

Muslima, N. Z., Ahmad, M., Heng, L. Y., and Saad, B. (2012) Optical biosensor test strip for the screening and direct determination of L-glutamate in food samples. Sensors and Actuators B: Chemical. 3; 161: 493-7.

O'Hara, P, J., Sheppard, P. O., Thógersen, H., Venezia, D., Haldeman, B. A., McGrane, V., Houamed, K. M., Thomsen, C., Gilbert, T. L., and Mulvihil, E. R. (1993) The ligand-binding domain in metabotropic glutamate receptors is related to bacterial periplasmic binding proteins l. Neuron 11: 41-52.

Ooij, C. V. (2009) Bacterial physiology: OppA's deep pockets. Nature Reviews Microbiology 7, 325

Ottersen, O. P., Laake, J. H., Reichelt, W., Haug, F. M., and Torp, R. (1996) Ischemic disruption of glutamate homeostasis in brain: quantitative immunocytochemical analyses. J Chem Neuroanat. 12(1):1-14. Review.

Ottersen, O. P., Zhang, N., and Walberg, F. (1992) Metabolic compartmentation of glutamate and glutamine: morphological evidence obtained by quantitative immunocytochemistry in rat cerebellum. Neuroscience. ;46(3):519-34.

Ottersen, O., P. and Storm-Mathisen J. (1984) Glutamate- and GABA-containing neurons in the mouse and rat brain, as demonstrated with a new immunocytochemical technique. J Comp Neurol. 1;229(3):374-92.

Pace, C. N., Vajdos, F., Fee, L., Grimsley, G., and Gray, T. (1995) How to measure and predict the molar absorption coefficient of a protein. Protein Sci. 4(11):2411-23.

Poetsch, A., Wolters D. (2008) Bacterial membrane proteomics Proteomics.; 8(19): 4100-22.

Qin, S., Evering, M., Wahono, N., Cremers, T. I. F. H. and Westering B. H. C. (2013) Monitoring Extracellular Glutamate in the Brain by Microdialysis and Microsensors. Neuromethods; 80: 153-177.

Quiocho F.A. (1991) Atomic structures and function of periplasmic receptors for active transport and chemotaxis. Curr. Opin. Struct. Biol., 1 pp. 922–933.

Quiocho, F. A., and Ledvina P. S. (1996) Atomic structure and specificity of bacterial periplasmic receptors for active transport and chemotaxis: variation of common themes. Mol. Microbiol., 20 pp. 17–25.

Raleigh, E. A., Murray, N. E., Revel, H., Blumenthal, R. M., Westaway, D., Reith, A. D., Rigby, P. W., Elhai, J., and Hanahan, D. (1988) McrA and McrB restriction phenotypes of some *E. coli* strains and implications for gene cloning. Nucleic Acids Res. 25;16(4):1563-75.

Riedel, G., and Reymann, K. G. (1996) Metabotropic glutamate receptors in hippocampal long-term potentiation and learning and memory. Acta Physiol Scand.;157(1):1-19.

Roland, T., and Milton H. S, J. (1993) Structural, Functional, and Evolutionary Relationships among Extracellular Solute-Binding Receptors of Bacteria. Microbiol. Mol. Biol. Rev. vol. 57 no. 2 320-346 1.

Rose, A. S., and Hildebrand, P. W. (2015) NGL Viewer: a web application for molecular visualization. Nucl Acids Res. 1, 43 (W1): W576-W579.

Rose, A. S., Bradley, A., R., Valasatava, Y., Duarte, J. M., Prlić, A., and Rose, P. W. (2016) Web-based molecular graphics for large complexes. ACM Proceedings of the 21st International Conference on Web3D Technology (Web3D '16): 185-186.

Rossi, D. J., Brady, J.D., and Mohr, C. (2007) Astrocyte metabolism and signaling during brain ischemia. Nat Neurosci.; 10(11): 1377-86.

Schneider, R., and Hantke, K. (1993) Iron-hydroxamate uptake systems in *Bacillus subtilis*: identification of a lipoprotein as part of a binding protein-dependent transport system. Mol Microbiol.; 8(1):111-21.

Schousboe, A., and Hertz, L. (1981) Role of astroglial cells in glutamate homeostasis. Adv Biochem Psychopharmacol. 27:103-13.

Shelton, M. K., and McCarthy, K. D. (1999) Mature hippocampal astrocytes exhibit functional metabotropic and ionotropic glutamate receptors in situ. Glia. 26(1):1-11.

Soldatkin, O., Nazarova, A., Krisanova, N., Borysov, A., Kucherenko, D., Kucherenko, I., Pozdnyakova, N., Soldatkin, A., and Borisova, T. (2015) Monitoring of the velocity of high-affinity glutamate uptake by isolated brain nerve terminals using amperometric glutamate biosensor. Talanta.; 135: 67-74.

Staiano, M., Baldassarre, M., Esposito, M., Apicella, E., Vitale, R., Aurilia, V., and D'Auria, S. (2010) New trends in bio/nanotechnology: stable proteins as advanced molecular tools for health and environment. Environ Technol.; 31(8-9): 935-42.

Steinhäuser, C., Gallo, V. (1996) News on glutamate receptors in glial cells. Trends Neurosci. ;19(8):339-45.

Stryer, L. (1965) The interaction of a naphthalene dye with apomyoglobin and apohemoglobin. A fluorescent probe of non-polar binding sites. J Mol Biol. 13(2):482-95.

Sundaram, R. S., Gowtham, L., and Nayak, B. S. (2012) The role of excitatory neurotransmitter glutamate in brain physiology and pathology. Asian J Pharm Clin Res; 5: 1-7.

Sutcliffe, I. C., and Russell, R. R. B. (1995) Lipoproteins of Gram-Positive Bacteria. Journal of Bacteriology, p. 1123–1128.

Sutcliffe, I. C., Tao, L., Ferretti, J. J., and Russell, R. R. B. (1993) Msme, a lipoprotein involved in sugar transport in *Streptococcus mutans*. J. Bacteriol. 175, 1853–1855.

Sutcliffe, I., L., Ferretti, J. J., and Russell, R. R. B. (1995) Lipoproteins of gram-positive bacteria. J. Bacteriol. 177, 1123-1128.

Tam, R., and Saier, M. H. Jr. (1993) Structural, functional, and evolutionary relationships among extracellular solute-binding receptors of bacteria. Microbiol Rev. 57(2):320-46. Review.

Tian, Y., Cuneo, M. J., Changela, A., Höcker, B., Beese, L. S., and Hellinga, H. W. (2007) Structure-based design of robust glucose biosensors using a *Thermotoga maritima* periplasmic glucose-binding protein. Protein Sci.; 16(10): 2240-50.

Trötschel, C., Kandirali, S., Diaz-Achirica P., Meinhardt, A., Morbach, S., Krämer, R., Burkovski, (2003) A. GltS, the sodium-coupled l-glutamate uptake system of *Corynebacterium glutamicum*: identification of the corresponding gene and impact on L-glutamate production. Appl Microbiol Biotechnol.; 60(6): 738-42.

Vernadakis, A. (1996) Glia-neuron intercommunications and synaptic plasticity Prog Neurobiol. Jun;49(3):185-214. Review.

Wang, X., Li, Y. H., Li, M. H., Lu, J., Zhao, J. G., Sun, X. J., Zhang. B., and Ye, J. L. (2012) Glutamate level detection by magnetic resonance spectroscopy in patients with post-stroke depression. Eur Arch Psychiatry Clin Neurosci.; 262(1): 33-8.

Wang, Y., Petty, S., Trojanowski, A., Knee, K., Goulet, D., Mukerji, I., and King, J. (2010) Formation of amyloid fibrils in vitro from partially unfolded intermediates of human gamma C-crystallin. Investigative Ophthalmology and Visual Science. 51:672–678.

Wicker, L., Lanier, T., Hamann, D., and Akahane, T. (1986) Thermal transitions in myosin-ANS fluorescence and gel rigidity. J Food Sci 51(6):1540–1543.

Zhang, G., Wang, L., Fu, P., and Hu, M. (2011) Mechanism and conforma- tional studies of farrerol binding to bovine serum albumin by spectroscopic methods. Spectrochim Acta Part A 82(1):424–431.